

University of Windsor

## Scholarship at UWindor

---

Electronic Theses and Dissertations

Theses, Dissertations, and Major Papers

---

1-1-1962

### An experimental study of natural convection heat transfer to non-Newtonian fluids in confined horizontal layers.

Carl C. St. Pierre  
*University of Windsor*

Follow this and additional works at: <https://scholar.uwindsor.ca/etd>

---

#### Recommended Citation

St. Pierre, Carl C., "An experimental study of natural convection heat transfer to non-Newtonian fluids in confined horizontal layers." (1962). *Electronic Theses and Dissertations*. 6317.  
<https://scholar.uwindsor.ca/etd/6317>

This online database contains the full-text of PhD dissertations and Masters' theses of University of Windsor students from 1954 forward. These documents are made available for personal study and research purposes only, in accordance with the Canadian Copyright Act and the Creative Commons license—CC BY-NC-ND (Attribution, Non-Commercial, No Derivative Works). Under this license, works must always be attributed to the copyright holder (original author), cannot be used for any commercial purposes, and may not be altered. Any other use would require the permission of the copyright holder. Students may inquire about withdrawing their dissertation and/or thesis from this database. For additional inquiries, please contact the repository administrator via email ([scholarship@uwindsor.ca](mailto:scholarship@uwindsor.ca)) or by telephone at 519-253-3000ext. 3208.

AN EXPERIMENTAL STUDY OF NATURAL CONVECTION HEAT TRANSFER  
TO NON-NEWTONIAN FLUIDS IN CONFINED HORIZONTAL LAYERS

A Thesis  
Submitted to the Faculty of Graduate Studies through the  
Department of Chemical Engineering in Partial Fulfilment  
of the Requirements for the Degree of  
Master of Applied Science at  
Assumption University of  
Windsor

by

CARL C. ST. PIERRE  
B.A.Sc., Assumption University of Windsor, 1961

Windsor, Ontario, Canada  
1962

**ASSUMPTION UNIVERSITY LIBRARY**

UMI Number: EC52496

### INFORMATION TO USERS

The quality of this reproduction is dependent upon the quality of the copy submitted. Broken or indistinct print, colored or poor quality illustrations and photographs, print bleed-through, substandard margins, and improper alignment can adversely affect reproduction.

In the unlikely event that the author did not send a complete manuscript and there are missing pages, these will be noted. Also, if unauthorized copyright material had to be removed, a note will indicate the deletion.

**UMI**<sup>®</sup>

---

UMI Microform EC52496

Copyright 2008 by ProQuest LLC.

All rights reserved. This microform edition is protected against unauthorized copying under Title 17, United States Code.

ProQuest LLC  
789 E. Eisenhower Parkway  
PO Box 1346  
Ann Arbor, MI 48106-1346

ABK7073

APPROVED BY:

John G. Guck

John G. Guck

John G. Guck

### ABSTRACT

The purpose of this work was to study the natural convection heat transfer of non-Newtonian fluids confined between horizontal plates. The apparatus used was similar to that employed by previous investigators (7), (24) and five different aqueous polymer solutions were used in the experimental work. In addition, heat transfer studies were also carried out using two different Newtonian fluids to assess the reliability and accuracy of the equipment.

The experimental results, expressed in terms of dimensionless quantities, were correlated by the method of least squares and yielded the following empirical expression:

$$N_{Nu} = 0.0832 N_{Ra}^{0.324} N_{PR}^{0.084} N^{1.75}$$

This expression is believed to be valid for both Newtonian and non-Newtonian fluids in the Rayleigh number range  $10^4$  to  $10^7$ .

The experimental range of the various dimensionless groups follows:

$$4.45 < N_{PR} < 13,800$$

$$2,470 < N_{Ra} < 7.09 \times 10^6$$

$$0.38 < N < 1.0$$

$$1.00 < N_{Nu} < 15.2$$

#### ACKNOWLEDGEMENTS

The author gratefully acknowledges the able direction of Dr. C. Tien, under whose suggestion this problem was undertaken. Thanks are due also to Mr. H. Y. Lo for his assistance in the determination of the physical constants, and to Mr. W. Lourette, who aided in the construction and layout of the heat transfer equipment. Financial assistance was provided by the National Research Council of Canada.

## TABLE OF CONTENTS

ABSTRACT	iii
ACKNOWLEDGEMENTS	vi
LIST OF TABLES	vii
LIST OF FIGURES	viii
CHAPTER I INTRODUCTION	1
CHAPTER II LITERATURE SURVEY	3
CHAPTER III THEORY	
A. Rheological Classification of Fluids	6
1. Newtonian Fluids	
2. Non-Newtonian Fluids	
a) Bingham Plastic	
b) Pseudoplastic Fluids	
c) Dilatant Fluids	
B. Natural Convection	10
1. Newtonian Fluids in Natural Convection	
2. Non-Newtonian Fluids in Natural Convection	
CHAPTER IV EXPERIMENTAL ARRANGEMENT AND PROCEDURE	
A. Apparatus	16
1. Heat Transfer Apparatus	
2. Physical Properties	
a) Rheological Properties	
b) Thermal Conductivities	
c) Densities and Coefficients of Thermal Expansion	
B. Experimental Procedure	20
1. Heat Transfer	
2. Physical Properties	
a) Rheological Properties	
b) Thermal Conductivities	
c) Densities and Coefficients of Thermal Expansion	
d) Heat Capacities	
C. Calibrations	24
1. Heat Transfer Apparatus	
2. Apparatus used for the Determination of Physical Properties	
a) Rotational Viscometer	
b) Thermal Conductivity Apparatus	
c) Pycnometer	

CHAPTER V	TEST FLUIDS	
A.	Solution Preparation	26
1.	Newtonian Fluids	
2.	Non-Newtonian Fluids	
B.	Test Fluid Properties	27
1.	Newtonian Fluids	
2.	Non-Newtonian Fluids	
a)	Carbopol 934	
b)	Methocel 65 H.G.	
c)	Carbose I.M.	
CHAPTER VI	RESULTS AND DISCUSSION	
A.	Physical Properties	30
1.	Rheological Properties	
a)	Carbopol 934	
b)	1% Methocel	
c)	0.5% Carbose I.M.	
2.	Thermal Conductivities	
3.	Densities and Coefficients of Thermal Expansion	
B.	Heat Transfer Results	36
CHAPTER VII	FUTURE WORK	46
NOMENCLATURE		47
REFERENCES		50
APPENDIX I		52
APPENDIX II		58
APPENDIX III		64
APPENDIX IV		68
APPENDIX V		77
APPENDIX VI		84
APPENDIX VII		91
VITA AUCTORIS		98



## LIST OF TABLES

<u>Table</u>		<u>Page</u>
1	Pycnometer Calibration Data	25
2	Thermal Conductivities of Polymer Solutions as Compared with Water	34
3	Correlation Results--Comparison with Work of O'Toole and Silveston	42
4	Viscometer Flow Data	59
5	Viscometer Flow Data	61
6	Thermal Conductivity Calibration Data: Water	62
7	Thermal Conductivity Calibration Data: 20% Ethylene Glycol	
8	Thermal Conductivity Apparatus Constants	63
9	Physical Properties of Water	68
10	Physical Properties of Glycerine	69
11	Physical Properties of Carbopol	70
12	Physical Properties of 1% Methocel	71
13	Physical Properties of 0.5% Carbose I.M.	71
14	Flow Curve Data: 1% Carbopol Solution	72
15	Flow Curve Data: 0.75% Carbopol Solution	73
16	Flow Curve Data: 0.50% Carbopol Solution	74
17	Flow Curve Data: 1% Methocel Solution	75
18	Flow Curve Data: 0.5% Carbose Solution	76
19	Heat Transfer Results: Water	77
20	Heat Transfer Results: Glycerine	78
21	Heat Transfer Results: 1% Methocel	79
22	Heat Transfer Results: 0.5% Carbopol	80
23	Heat Transfer Results: 0.5% Carbose	81
24	Heat Transfer Results: 0.75% Carbopol	82
25	Heat Transfer Results: 1% Carbopol	83

## LIST OF FIGURES

<u>Figure</u>		<u>Page</u>
1	Flow Curves for Time Independent Non-Newtonian Fluids	9
2	Flow Behavior Index--Aqueous Polymer Solutions	31
3	Consistency Index--Aqueous Polymer Solutions	32
4	Thermal Conductivity--Aqueous Polymer Solutions	35
5	Thermal Expansion Coefficients--Aqueous Polymer Solutions	37
6	Experimental Data Points	39
7	Experimental Data Correlation	40
8	Determination of Exponent C	41
9	Final Experimental Data Correlation	43
10	Heat Transfer Apparatus Detail	91
11	Schematic--Heat Transfer Setup	93
12	Thermal Conductivity Apparatus Detail	95
13	Schematic--Thermal Conductivity Apparatus	96

## CHAPTER I

### INTRODUCTION

The study of non-Newtonian technology has become increasingly important in recent years due to the increasing emergence of non-Newtonian fluids such as pulps, molten plastics, emulsions, etc., in a large variety of industrial processes. In particular, momentum and heat transfer to a non-Newtonian fluid in motion have been extensively studied and lead to solutions of a number of more simple and common classical hydrodynamics problems. Reviews of these studies have been made by Metzner (19) and others (5), (6), (29), (30).

Little attention, however, has been given to the study of free convective heat transfer to non-Newtonian fluids with the exception of a recent paper by Acrivos (1). The lack of experimental study is probably due to the usual high viscosities of non-Newtonian fluids and the reversion to Newtonian behavior of some of these fluids which occurs at very high and very low shearing rates--and low shearing rates of the order  $0.5-1.0 \text{ sec}^{-1}$  exist in natural convection.

An interesting starting point for the study of natural convection heat transfer has been the investigation of the Bénard cells which occur when a fluid is heated uniformly from below or cooled from above. The study of this problem led Rayleigh to formulate a new dimensionless number, i.e.  $N_{Ra} = N_{PR} \cdot N_{GR}$ , whose critical value indicates the onset of convection and also the dimensionless

group which can be used to correlate the experimental results of natural convection heat transfer. By the same analogy the problem of Benard seemed to be a logical starting point for a study of natural convective heat transfer to non-Newtonian fluids.

The problem studied in this thesis was resolved into two main divisions:

- i. to experimentally investigate the effects of non-Newtonian behavior on the phenomena of natural convection; and
- ii. to find suitable dimensionless groups which can satisfactorily correlate the experimental data.

The desired results of the study of this simple problem of natural convective heat transfer to non-Newtonian fluids in confined horizontal layers was that the proper form of the generalized groups would be discovered which can be used for the correlation of all natural convection heat transfer data.

## CHAPTER II

### LITERATURE SURVEY

The first experimental investigations of the instability of a fluid heated uniformly from below or cooled from above were made by Thompson (28) in 1881 and Bénard (2) in 1900. Later, their experiments were extended and repeated and these results may be briefly summarized as follows:

- a) In order that convection should take place, the temperature gradient must reach a critical value dependent on the depth and physical properties of the fluid;
- b) The convective motion tends towards a regular hexagon pattern;
- c) The size of the cell is fixed by the depth and physical properties of the fluid.

In 1916, Lord Rayleigh (15) obtained a theoretical formulation of the experimental results observed by Bénard. He formulated the flow equations for a discrete disturbance in the fluid and determined the conditions under which the disturbance would amplify and cause the layer to become unstable. This he found to occur at a critical value of the dimensionless group bearing his name:

$$N_{Ra} = \frac{g\beta\Delta T L^3}{\alpha U} \quad (2.1)$$

which can also be written as the product of the Prandtl number  $U/\alpha$  and the Grashof number

$$N_{GR} = \frac{g\beta\Delta T L^3}{U^2} \quad (2.2)$$

Rayleigh's theory was later refined, notably by Jeffreys (10) in 1930 and Low (16) who found the critical value of the Rayleigh number to be 1,709 and 1,704 respectively. This critical value was for a fluid system bounded by infinite, rigid conductors.

Various experimental investigations of the convective motion between horizontal surfaces followed the work of Rayleigh and Low. The first of these was by Schmidt and Milverton (25) in 1935, designed to test the theoretical conclusions of Rayleigh's and Jeffreys', concerning the conditions necessary for the onset of convection in a fluid heated from below. They observed a change in the heat transported through the fluid at the transition to cellular motion and found that the point of transition was in agreement with theory. In 1938 Schmidt and Saunders (26) reported a second transition in the heat transport accompanied by a change from laminar to turbulent motion. They also observed the ratios of the heat transported by the turbulent convection to that which would have been transported by conduction alone in a limited range of the boundary parameters near the point of transition. In 1946 Jakob (9) correlated the data on air of Mull and Reiher (21) which was confirmed and extended by De Graaf and Van Der Held (4).

Malkus (17) found six discrete transitions in the slope of the heat-transport curve between Rayleigh numbers of 1700 and  $10^6$  using water and acetone as fluids. Shortly afterwards Globe and Dropkin (7) using water, silicone oils and mercury experimentally investigated the turbulent region of convective heat transfer and found all the liquids investigated could have their heat transfer coefficients expressed by:

$$N_{Nu} = 0.069 (N_{Ra})^{1/3} (N_{PR})^{0.074} \quad (2.3)$$

Schmidt and Silveston (24) employing five different liquids and optical observations, found three distinct convection regimes to exist and by a plot of Nusselt number versus Rayleigh number found for the turbulent region that heat transfer is approximated by the simple relation:

$$N_{Nu} = 0.094 (N_{Ra})^{1/3} \quad (2.4)$$

O'Toole and Silveston (22) correlated the work of Stumpf(27), De Graaf (4), Globe (7), Mull and Reiher (21) and Schmidt and Silveston (24) by means of step-by-step multiple regression on the assumption that the expression for heat transfer is linear in its logarithmic form. Their results for the three regimes can be expressed as follows:

$$N_{Nu} = 0.00238 (N_{Ra})^{0.816} \quad 1700 < N_{Ra} < 3500 \quad (2.5)$$

$$N_{Nu} = 0.229 (N_{Ra})^{0.252} \quad 3500 < N_{Ra} < 10^5 \quad (2.6)$$

$$N_{Nu} = 0.104 (N_{Ra})^{0.305} (N_{PR})^{0.084} \quad 10^5 < N_{Ra} < 10^9 \quad (2.7)$$

To the author's knowledge, there is no theoretical or experimental work published on the phenomena of natural convection when a non-Newtonian fluid is heated uniformly from below or cooled from above.

## CHAPTER III

### THEORY

#### A. Rheological Classification of Fluids

A discussion of the various types of non-Newtonian fluids has been presented in many books (3, 8, 19, 20), and for this reason only a brief description will be included here for the purpose of comparison of data presented in this thesis with other types of fluids.

##### 1. Newtonian Fluids

Newtonian fluids are those which exhibit a direct proportionality between shear stress and shear rate in the laminar flow region.

Thus

$$\tau = \mu \left( \frac{du}{dy} \right) \quad (3.1)$$

where  $\mu$  is the constant of proportionality called viscosity. The "flow curve" or diagram relating shear stress to shear rate is a straight line having slope equal to  $\mu$ . Alternately, if the flow curve is plotted using logarithmic coordinates, all Newtonian fluids have the same slope (unity) while the intercept at a shear rate of unity gives the value of  $\mu$ .

##### 2. Non Newtonian Fluids

Non-Newtonian fluids are those for which the flow curve plotted using logarithmic coordinates deviates from linearity and the viscosity is now not only a function of temperature and pressure as for



Newtonian fluids, but is also a function of one or more of the following:

- i) rate of shear;
- ii) apparatus shape in which the fluid is contained;
- iii) the previous history of the fluid.

These non-Newtonian fluids may be classified into three broad groups:

- i) fluids for which the rate of shear at any point is some function of the shearing stress and is independent of time or duration of shear;
- ii) more complex systems in which the relation between shearing stress and shearing rate is dependent on the duration of shear or on its previous history;
- iii) systems having characteristics of both solids and fluids which exhibit elastic recovery after deformation.

Since in this thesis only the first classification of fluid was encountered, the discussion will be restricted to these time-independent non-Newtonian fluids.

### 3. Time Independent Non-Newtonian Fluids

Time independent non-Newtonian fluids fall into three distinct groups depending on the nature of the function:

$$\frac{du}{dy} = f(\tau) \quad (3.2)$$

They are the following:

- a) Bingham plastics
- b) Pseudoplastic fluids
- c) Dilatant fluids

a) Bingham Plastics. A Bingham plastic is characterized by a flow curve which is a straight line having intercept  $\tau_y$  on the shear stress axis. This yield stress ( $\tau_y$ ) must be exceeded before flow starts and the rheological equation for a Bingham plastic may be written:

$$\tau - \tau_y = \mu_p \left( \frac{du}{dy} \right) \quad (3.3)$$

where  $\mu_p$  is the plastic viscosity. Common examples are slurries, paints, toothpaste, sludges and drilling muds.

b) Pseudoplastic Fluids. This is the most important classification, since it is the one into which the majority of non-Newtonian fluids fall. This type shows no yield value and the typical flow curve for these fluids exhibits flow curves having slopes between zero and unity. The power law model of Ostwald is the most widely used expression relating shear stress to shear rate. This may be written as:

$$\tau = K \left| \frac{du}{dy} \right|^{N-1} \frac{\partial u}{\partial y} \quad (3.4)$$

where K and N are constants. The constant K (consistency index) is a measure of the consistency of the fluid and can be considered analogous to the viscosity while the exponent N (flow index) is a measure of the degree of non-Newtonian behavior at its value ranges from zero to one. The dimensions of K depend upon N and this fact has led to many objections to the power law model.

The apparent viscosity ( $\mu_A$ ), which is the ratio of shearing stress to shearing rate, can be expressed in terms of N for the power law fluid:

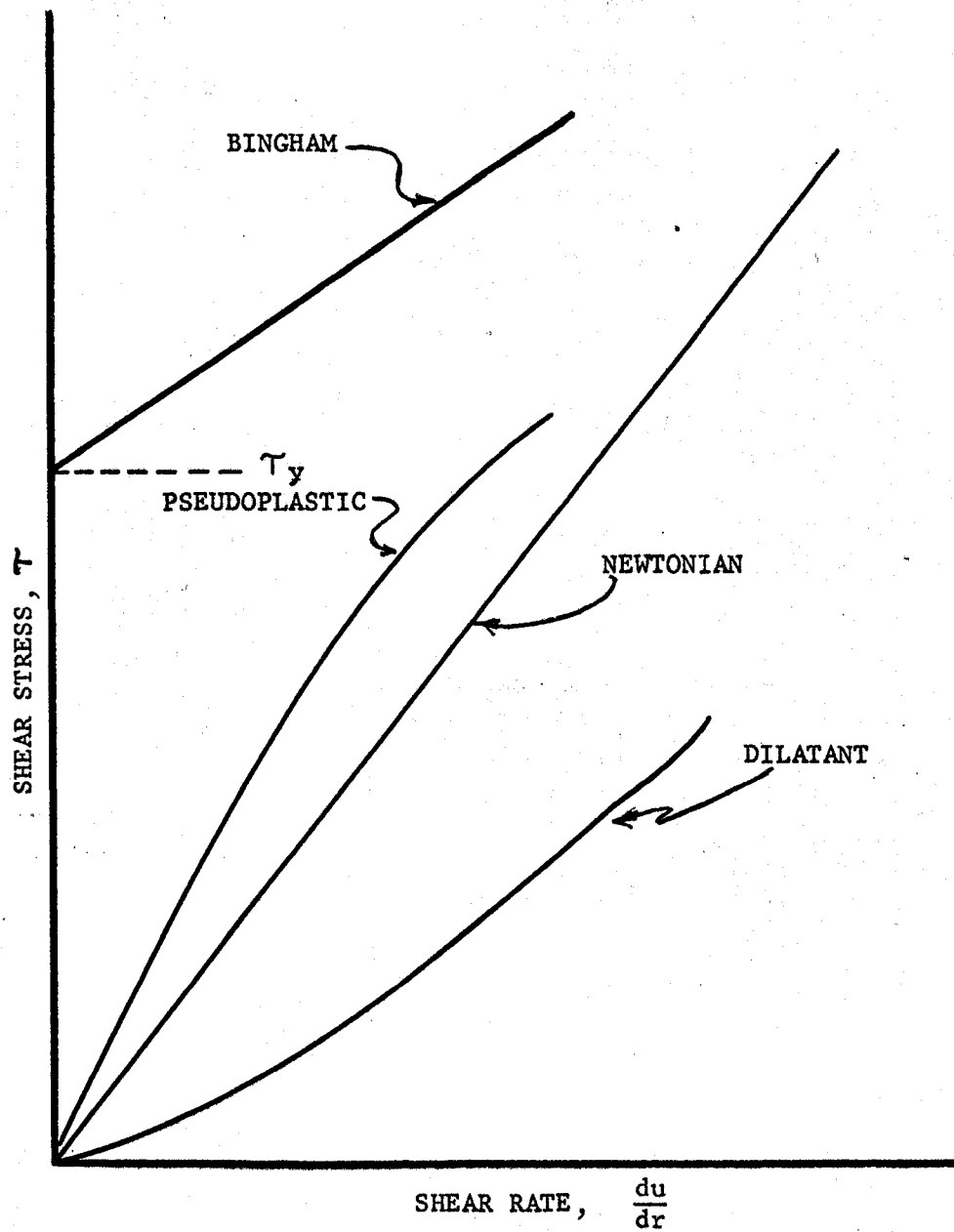


Fig. 1. Flow curves for various types of time-independent non-Newtonian fluids.

$$\mu_A = \frac{\tau}{\left(\frac{du}{dy}\right)} = K \left| \frac{du}{dy} \right|^{N-1} \quad (3.5)$$

and since  $N < 1$  for pseudoplastics the apparent viscosity decreases as the rate of shear increases.

Other empirical equations have also been proposed to describe pseudoplastic behavior and for a list of these any of the referenced texts at the beginning of this chapter may be consulted.

c) Dilatant Fluids. This type of fluid also has no yield stress, but the typical flow curves for these fluids have slopes which are greater than unity. The power law equation is often applicable for this case and the apparent viscosity increases with increasing rates of shear for this type of fluid. This type of behavior was originally discovered by Osborne Reynolds in suspensions having high solids content.

#### B. Natural Convection

The application of the principle of similarity to heat transfer often leads to results which are useful in the representation of results of experimental research and the dimensionless parameters obtained in the form of products of powers of dimensioned quantities yield meaningful parameters. These characteristic dimensionless parameters can be obtained in two ways:

- i) normalization of the differential equations of fluid flow and heat transfer by the introduction into the equations of suitable power products of the principal quantities;
- ii) the more general approach of dimensional analysis.

## Newtonian Fluids in Natural Convection

The governing dimensionless parameters for natural convection can be found by the application of the principle of similarity in either of the above methods and the method of dimensional analysis is worked out in detail in Appendix I. For free convection the buoyancy force caused by changes in volume associated with temperature differences must be introduced into the momentum equation as a body force. For example, a fluid layer heated from below suffers a density decrease or change in specific volume and as a result experiences a buoyancy force. Expressing the change in specific volume in terms of the coefficient of thermal expansion:

$$\beta = \frac{1}{v_s} \left( \frac{\partial v_s}{\partial \theta} \right)_p \quad (3.6)$$

and denoting the temperature difference between the hotter particle and that of the colder surroundings as  $\Delta \theta$ , the buoyancy force per unit volume becomes:

$$\vec{G} = \beta \rho \vec{g} \Delta \theta \quad (3.7)$$

Inserting this body force into the momentum equation and applying the principle of similarity the following dimensionless parameters are obtained:

$$N_{GR} = \frac{g \beta \Delta \theta L^3}{v^2} \quad (3.8)$$

$$N_{PR} = \frac{v}{\nu} \quad (3.9)$$

$$N_{NU} = \frac{h L}{K} \quad (3.10)$$

which can be grouped to describe heat transfer in free convection by

the equation:

$$N_{Nu} = f(N_{GR}, N_{PR}) \quad (3.11)$$

If the acceleration terms in the momentum equation are neglected, we obtain the equation of "creeping motion" and for this case the equations yield in addition to the Nusselt number only one dimensionless parameter having the form:

$$N_{Ra} = \frac{g \beta \Delta \theta L^3}{\nu \alpha} = N_{GR} N_{PR} \quad (3.12)$$

and equation (6) is replaced by the relation:

$$N_{Nu} = f(N_{GR}, N_{PR}) = f(N_{Ra}) \quad (3.13)$$

By application of the method of dimensional analysis results identical to the above can be obtained. (Appendix I)

#### Non-Newtonian Fluids in Natural Convection

For non-Newtonian fluids the quantities affecting the problem of free convection are the same as those for Newtonian fluids, except the viscosity term which must be defined to include non-Newtonian effects. Assuming the power law model of Ostwald the relation between shear-stress and shear-rate is given by:

$$\tau = K \left( \frac{du}{dy} \right)^N \quad (3.14)$$

where  $N$  is the "flow behavior index" and  $K$  is called the "consistency index". The consistency index is analogous to the viscosity term for Newtonian fluids and, as the name indicates, it characterizes the consistency of the fluid.

Thus the quantities which can be reasonably expected to affect the problem of free convection are the following:

<u>Quantity</u>	<u>Symbol</u>	<u>Dimensions</u>
Length	L	ft [L]
Buoyant Acceleration	$g \beta$	ft/sec <sup>2</sup> °F [LT <sup>-2</sup> θ <sup>-1</sup> ]
Density	$\rho$	lb M/ft <sup>3</sup> [ML <sup>-3</sup> ]
Thermal Conductivity	k	Btu/ft(sec)°F [QL <sup>-1</sup> T <sup>-1</sup> θ <sup>-1</sup> ]
Temperature Difference	$\Delta \theta$	°F [θ]
Specific Heat	$C_p$	Btu/lbM°F [QM <sup>-1</sup> θ <sup>-1</sup> ]
Heat Transfer Coefficient	h	Btu/ft <sup>2</sup> sec°F [QL <sup>-2</sup> θ <sup>-1</sup> T <sup>-1</sup> ]
Consistency Index	K	lb <sub>M</sub> /ft(sec) <sup>2-N</sup> [ML <sup>-1</sup> T <sup>N-2</sup> ]

The solution of our problem should contain dimensionless parameters in the form of products of powers of the various variables involved. Each of the parameters must be of the form;

$$L^{x_1} (g\beta)^{x_2} \rho^{x_3} k^{x_4} k^{x_5} (\Delta\theta)^{x_6} C_p^{x_7} h^{x_8} \quad (3.15)$$

where  $x_1, x_2, \dots, x_N$  denote exponents which are unknown so far. Writing down the dimensions of the above product we obtain:

$$L^{x_1} [L T^{-2} \theta^{-1}]^{x_2} [ML^{-3}]^{x_3} [ML^{-1} T^{N-2}]^{x_4} [QL^{-1} T^{-1} \theta^{-1}]^{x_5} [\theta]^{x_6} \\ [QM^{-1} \theta^{-1}]^{x_7} [QL^{-2} \theta^{-1} T^{-1}]^{x_8} \quad (3.16)$$

In order for the product to be dimensionless, we can equate the dimensions of time, length, etc., respectively to zero and obtain five equations for the eight unknown exponents.

For the dimension of length [L]:

$$x_1 + x_2 - 3x_3 - x_4 - x_5 - 2x_8 = 0 \quad (3.17)$$

For the dimension of time [T]:

$$-2x_2 - 2x_4 + Nx_4 - x_5 - x_8 = 0 \quad (3.18)$$

For the dimension of heat [Q]:

$$x_5 + x_7 + x_8 = 0 \quad (3.19)$$

For the dimension of temperature [ $\theta$ ]:

$$-x_2 - x_5 + x_6 - x_7 - x_8 = 0 \quad (3.20)$$

For the dimension of mass [M]:

$$x_3 + x_4 - x_7 = 0 \quad (3.21)$$

Choose  $x_6$ ,  $x_7$  and  $x_8$  as our arbitrary exponents and express the remaining five exponents in terms of these three.

The following power product results:

$$L^{x_8 - x_6 + 2x_7 + \frac{2(x_7 - 2x_6)}{N-2}} (g\beta)^{x_6} (\Delta\theta)^{x_6} e^{\frac{(N-2)x_7 - 2x_6 + x_7}{N-2}} \\ K^{\frac{2x_6 - x_7}{N-2}} k^{-x_7 - x_8} c_p^{x_7} h^{x_8} \quad (3.22)$$

The three arbitrary exponents may be eliminated by setting each one in turn equal to one while simultaneously setting the remaining two equal to zero. For  $x_6 = 1$  and  $x_7 = x_8 = 0$  we obtain:

$$N_{GR} = \frac{L^{\frac{N+2}{2-N}} g \beta \Delta \theta}{\left[ \frac{K}{e} \right]^{\frac{2}{2-N}}} \quad (3.23)$$

also for  $x_7 = 1$ ;  $x_6 = x_8 = 0$ :

$$N_{PR} = \frac{c_p e}{k} \left[ \frac{K}{e} \right]^{\frac{1}{2-N}} L^{\frac{2N-2}{N-2}} \quad (3.24)$$



and finally for  $x_8 = 1$ ,  $x_6 = x_7 = 0$ :

$$N_{Nu} = \frac{h L}{k} \quad (3.25)$$

The required function thus contains three dimensionless arguments and has the now familiar form:

$$N_{Nu} = f(N_{GR}, N_{PR}) \quad (3.26)$$

where the product  $N_{GR} N_{PR}$  yields the dimensionless group called the Rayleigh number.

$$N_{Ra} = \left[ \frac{C_p g \beta \Delta \theta}{k} \right] \left[ \frac{\rho^{\frac{N-3}{N-2}} L^{\frac{4-N}{2-N}}}{K \frac{1}{2-N}} \right] \quad (3.27)$$

The above dimensionless numbers, which have been generalized using the Ostwald power law model for non-Newtonian fluids, reduce to the usual expressions for Newtonian fluids when  $N=1$  and  $K = \mu$ .

Thus by virtue of our dimensional analysis, we would expect an experimental correlation of the form:

$$N_{Nu} = A N_{Ra}^a N_{PR}^b N^c \quad (3.28)$$

CHAPTER IV  
EXPERIMENTAL ARRANGEMENT AND PROCEDURE

A. APPARATUS

Heat Transfer Apparatus

The theoretical model to be approximated by this experiment is that of a fluid contained between two infinite horizontal conducting surfaces separated by a fixed distance and imposed at fixed temperatures.

The actual experiment must then be designed to permit a close approximation of the theoretical model. The influence of the vertical boundaries which confine the fluid and the local fluctuations of the boundary temperature due to the finite conductivity and heat capacity of the boundary material must be minimized and determined. Also, considerable caution must be taken that heat losses or gains from the surrounding region or from the heat capacity of the necessary equipment are accounted for.

Figs. 10 and 11, Appendix VII, diagram the experimental apparatus, which consisted of a right circular plexiglass cylinder with an O.D. of six inches and an I.D. of four inches. The two horizontal conducting surfaces were identical in construction and consisted of a (1/16 inch) thin bakelite sheet 2 1/2 inches in diameter, sandwiched between a two inch copper plate and a smaller (1/4 inch) copper plate. The smaller plate which contacted the experimental fluids was carefully finished and chrome plated.

The fluid container is the cylindrical space between the two conducting surfaces, and it has an I.D. of four inches and a height of one inch.

To prevent fluid leakage from this space, "O"-ring seals were employed. Heat was removed from the upper conducting surface by circulating cold water through the larger copper block--the cold water temperature could be preset and regulated. The lower conducting surface had two 100-watt heaters sealed in it and electrical input to the heaters was measured by use of a wattmeter and voltmeter. To insure constant voltage, a voltage regulator was connected into the electrical circuit and the voltage to the heaters was varied by means of a "Variac".

To determine the temperature of the conducting surfaces, copper-constantan thermocouples were imbedded in each of the plates with the thermocouples measuring the face temperature of the plates adjacent to the fluid, being only 0.03 inches from the liquid surface. The apparatus was mounted on a levelling platform which, when used with the level, insured the whole apparatus was horizontal before each run.

In order to minimize heat losses from the vertical insulating walls, the whole apparatus was covered by an inverted Dewar flask. A doughnut-shaped ring of one inch thickness, which was placed around the apparatus at the location of the liquid container, served two purposes:

- i) supported the inverted Dewar flask;
- ii) provided an excellent insulation between the upper and lower half of the spaces formed by the ring.

To insure a good seal between the insulating ring and Dewar flask, an oversized felt ring was glued to the insulating ring and this aided the buildup of a layer of insulating air for the upper, cold half and the lower, warm half. During the experimental runs, the insulating air layer temperature closely approximated that of the conducting surface it was surrounding, and any heat losses or heat gains were found to be compensating and could be neglected. Also, it was felt that a guard heater was not required for the bottom hot plate, since insulation was provided by 2 1/4 inches of plexiglass, 1/2 inch of felt and 3/4 inch of wood. The experimental heat transfer apparatus used in this investigation was believed to closely approximate the theoretical model required for this experiment.

#### Physical Properties

a) Rheological Properties. There are two basic and distinct methods for the determination of the rheological properties of time-independent fluids:

- i) Direct determination of the relationship between shearing stress and shearing rate by use of a laboratory viscometer, usually of the coaxial cylinder or cone and plate type.
- ii) Inference of the relationship between shearing stress and shearing rate from measurements on the pressure drop and volumetric flow rate in a straight pipe or capillary tube.

The first method has an important advantage, that measurements of the actual physical properties of the fluids are made and used to interpret the heat transfer data. Also, for natural convection the shearing rates are of the order of magnitude of  $0.1-1.0 \text{ sec}^{-1}$  (1)

and the viscometer employed had to be capable of accurate measurements of the rheological properties in this range. For the above reasons, a coaxial cylinder viscometer was used, manufactured by the Brookfield Engineering Laboratories. The L.V.T. model had eight speed ranges which permitted a ratio of maximum to minimum shear rates of 200:1; also, by use of the U.L. Adapter and very low speeds, an accurate determination of the rheological properties in the shear rate range of  $0.5 \text{ sec}^{-1}$  was made possible. The model of viscosimeter was guaranteed to be accurate to within 1% of full scale value, and to have a reproducibility of 0.2%.

The U.L. Adapter furnished with the model consisted of a precision cylindrical spindle rotating inside an accurately machined tube which held a sample 25 ml. in volume, and this adapter was employed for all test fluids except the 1% Carbopol.

b) Thermal Conductivities. Since the test fluids tended to solvate in the liquid, the thermal conductivities were evaluated experimentally. The thermal conductivity apparatus was of the cylindrical type which had been successfully used by Riedel (25).

The apparatus consisted of two concentric cylinders as diagrammed in Figs. 12 and 13, Appendix VII. An electrical heater located within the inner cylinder provided an accurately measured constant rate of heat which penetrated through the liquid lying within the annular gap and out into the outer cooling cylinder or block. Heat was conducted away from the outer block by twelve evenly spaced copper wires whose ends were submerged in an ice-water mixture. Since the rate of heat conduction from the outer cylinder exceeded that being produced

within the inner cylinder, a compensating heating element was wound over the cooling cylinder underneath the point where the copper wires were connected. By careful regulation of the compensating heater, the temperature of the outer cylinder was maintained constant.

Temperatures of the respective blocks were determined by means of copper-constantan thermocouples embedded in their surfaces and the heaters were constructed from 30-gauge copel heating wire. Thus, by determination of the temperature difference between the heating and cooling cylinders and the rate of heat input at steady state conditions, the desired information for the determination of thermal conductivities was known.

c). Densities and Coefficients of Thermal Expansion. The densities of all the test fluids were determined by use of a pycnometer and a constant temperature bath. No difficulty was encountered in placing the fluid in the pycnometer nor was there any noticeable restriction on the expansion of the fluid as the temperature was increased. By elementary calculations, the coefficient of thermal expansions of each of the fluids was easily determined.

#### B. Experimental Procedure

##### Heat Transfer

All heat transfer measurements were made at steady-state conditions, which were indicated by the continuous temperature recorder, and equilibrium was considered established when readings remained constant for at least one hour. Liquids were degassed before use and the container was filled with the appropriate liquid, ensuring no air pockets remained at the underside of the top plate. The layer was

inspected for vapor spaces after each run, and each run lasted approximately three hours. It was found that the more viscous fluids took a longer time interval to reach steady-state conditions than the less viscous fluids.

The electrical input was preset by use of the Variac to a predetermined level, and the recording potentiometer started. Simultaneously, cold water was circulated throughout the top plate and the cold water temperature was also preset to a predetermined level by use of a thermostat. After the recording potentiometer indicated that steady-state had been reached, the thermocouple temperatures were read and recorded, using a precision potentiometer.

The heat flux through the liquid layer was the power supplied to the heating elements corrected for watt-meter losses and heat transferred through the plexiglass spacer. The arithmetic average of the hot and cold surface temperatures was used as the mean temperature of the fluid and all the dimensionless numbers were based on this temperature.

All thermocouple temperatures were recorded including those indicating the temperatures of the insulating air layers; also recorded were the wattmeter and voltmeter readings.

The A. C. power supply entered through a fused main switch and then to a timer switch which electrically controlled the whole experimental setup and allowed starting and stopping of the experimental work at any desired time.

#### Physical Properties

- a) Rheological Properties. All rheological properties of the

test fluid were determined after the liquids had been degassed and also before and after each run. No appreciable difference existed in the viscosities of the test fluids when measured before and after each test.

A 25 ml. sample of fluid was carefully pipetted into the test container and then the test container was immersed in a constant temperature bath. The bath temperature was regulated to one-tenth of a degree by use of a calibrated thermometer and thermostat accurate to  $\pm 0.05$  of a degree centigrade when properly preset. The test fluid temperature was allowed to come to steady-state conditions and then the shearing rate and shearing stress values were recorded until two consecutive readings gave results within the reproducibility of the viscometer. The bath temperature was then reset and the above process repeated to obtain the flow curves over both the maximum possible shear rate range and the desired temperature range. The non-Newtonian flow curves were calculated and plotted using the method of Krieger and Maron (11) which was found to be applicable to concentric cylinder viscometers in which the inner cylinder rotates and the outer cylinder is stationary. The discussion of the method of Krieger and Maron for this particular case is included in Appendix III.

b) Thermal Conductivities. A sample of the degassed test fluid was flushed through the test chamber and then the chamber was filled and the level adjusted on the burets for both the entrance and exit ports. The ice bath was filled and the ends of the cooling coils immersed. The inner cylinder was heated to a preset level and when



steady-state was approaching, the guard heater on the outer cylinder was carefully set to insure that constant temperature remained in both the inner and outer cylinders. After steady-state was maintained, the temperature difference across the fluid gap was recorded by use of a precision potentiometer and the power supplied to both the inner cylinder and compensating heater were recorded. From these data, the thermal conductivities could be easily determined.

c) Densities and Coefficients of Thermal Expansion. In order to determine the variation of density of the test fluids with temperature, a pycnometer was used. The pycnometer was first calibrated, using distilled water to calculate the volume, and then samples were introduced at a temperature lower than that at which the determination was made. The pycnometer was then suspended in the constant temperature bath until the temperature of the solution reached steady-state as determined by the absence of formation of any additional fluid on the pycnometer capillary stem. Then, by weighing the pycnometer with the solution and knowing the actual weight and volume of the pycnometer, the densities could be very easily calculated. The experimental densities were very slightly higher than that of water and from a plot of specific volume vs. temperature, the variation of volume with temperature was determined graphically and, knowing this value, the coefficient of thermal expansion was easily calculated. The expansion coefficient agreed very closely with that for water and, in all calculations, the expansion coefficient of water was used. (Fig. 5)

d) Heat Capacities. All the heat capacities of the test solutions were assumed equal to that of water, on the basis of the work performed by Vaughn (29) on similar solutions.

### C. Calibrations

#### Heat Transfer Apparatus

In order to check the reliability and accuracy of the data obtained using the experimental heat transfer apparatus, distilled water was employed. Water served as a good calibration liquid for two reasons:

- i) Extensive physical data was readily available.
- ii) Previous experimental data for water determined on similar equipment was available.

The data obtained for the water runs agreed very closely with that of previous workers (7, 24, 27) with the average deviation in the Nusselt number being  $+8\%$  of the calculated Nusselt number, using the correlated data of O'Toole and Silveston (22) in the  $N_{Ra}$  range of  $10^5$  to  $10^7$ .

Indeterminate errors in the experimental runs were small and the precision and reproducibility were high. The main sources of indeterminate errors were:

- i) determination of heat losses;
- ii) edge effects of wall;
- iii) location of thermocouples slightly under, not on the surface;
- iv) basing calculations of dimensionless groups on the arithmetic mean temperature.

#### Apparatus Used for the Determination of Physical Properties

a) Rotational Viscometer. Two N.B.S. Oils were used to calibrate the viscometer in order to determine the equivalent bob

length and to correct for end effects. Sample calculations of the equivalent lengths and tabulated data is listed in Appendix II. For the coaxial cylinder viscometer (U.L.Adapter) the obtained equivalent bob length was 3.62 inches as compared to an actual length of 3.57 inches. Spindle No. 1 was also calibrated to obtain an equivalent bob length of 3.01 inches as compared to the actual length of 2.56 inches.

b) Thermal Conductivity Apparatus. Redistilled water and a 20% aqueous ethylene glycol solution were used for the calibration of the thermal conductivity apparatus. The apparatus constants and tabulated calibration data are listed in Appendix II.

c) Pycnometer. The volume of the pycnometer was determined using redistilled water. The volume was calculated by weighing the vessel filled with water at fixed temperatures maintained to  $\pm 0.05$  C and using the corresponding density obtained from tables (14). The calibration data is listed in Table 1:

Table 1

Pycnometer Calibration Data

Pycnometer Weight = 22.1940 gms.

T C	Water Weight Gms.	Water Density Gms/MI	Pycnometer Volume Mls.
25.8	50.2716	0.996836	50.431
30.0	50.2158	0.995646	50.435

The arithmetic mean average of 50.433 mls. was used as the pycnometer volume in all density calculations.

## CHAPTER V

### TEST FLUIDS

The primary criteria for the selection of test fluids used in this study were that they exhibit a wide range of non-Newtonian behavior in the low shearing-rate range characteristic of natural convection, and also that they be free from any viscoelastic and time-dependent effects. The calibrating fluids (water and glycerine) were chosen primarily because of the availability of extensive data on their physical properties.

#### A. Solution Preparation

##### Newtonian Fluids

Water and glycerine were used as test fluids and the water required no actual preparation other than that it was distilled and degassed before being placed in the heat transfer apparatus. However, more care had to be exercised in the case of glycerine, due to its hygroscopic behavior. A reagent grade glycerine was used which was degassed at 105°C to insure the removal of trace impurities of water. After being placed in the heat transfer apparatus, the filling holes to the liquid reservoir were sealed off by means of silica gel in thistle tubes, and the inverted Dewar flask also was packed with silica gel to absorb any condensation.

##### Non-Newtonian Fluids

Since all the non-Newtonian solutions prepared involved the

dissolving of hydrophilic polymers (which dissolve by the mechanism of hydration and swelling) all solutions were prepared in the same manner. The mechanism of dissolution was very different from that of common salts and, in order to obtain optimum solution rates, the procedure outlined in the Dow "Methocel" Handbook (18) was followed in preparing the solutions. Essentially this method involved the process of wetting the material at elevated temperatures (80-90°C) while stirring rapidly and then cooling the solution to a much lower temperature (10-15°C).

#### B. Test Fluid Properties

##### Newtonian Fluids

The physical properties of water used in the calculation of the dimensionless groups for this experiment are listed in the Appendix IV. The glycerine used in the experimental work was a high grade, laboratory reagent purchased from the British Drug Houses (Canada) Limited (Lot 21423). From the actual physical density of 1.255-1.260 gm/ml (at 20°C) for the glycerine, and using the table of densities of aqueous glycerol solutions (14), the maximum impurity which could be present as water was found to be 0.39% (if water was the only impurity). Since the presence of water affects the viscosity of glycerine most markedly, the table of absolute viscosities of aqueous glycerol solutions (14) was checked to find the maximum possible effect of water. It was found that the maximum error in the viscosity would be 4% due to the presence of water, but due to the precautions employed the amount of water in the glycerine should have

been lower than that theoretically possible.

The physical properties of glycerine are listed in Appendix IV.

#### Non-Newtonian Fluids

Three different non-Newtonian systems were used as test fluids, their trade names being Carbopol (B. F. Goodrich), Methocel (Dow) and Carbose (Wyandotte Chemical).

a) Carbopol 934. Three different weight percent aqueous solutions of Carbopol 934 were used. Carbopol, a trade name of the B. F. Goodrich Company, is a carboxy-polymethylene whose exact structure has not yet been revealed. The solutions were used in their un-neutralized form, having a pH of approximately 3, since the neutralization step would have increased the viscosities to such an extent as to damp out natural convection almost completely.

An examination of the flow curves revealed that the solutions conformed to the power law model over the range of shear rates studied and the flow behavior index ranged from 0.3 to 0.9. All the other physical properties which were experimentally determined have been listed in Appendix IV.

b) Methocel 65 H.G. Methocel, manufactured by the Dow Chemical Company, is a hydroxy-propyl methylcellulose formed by the substitution of varying ratios of propylene glycol ether to methoxyl substitution on the anhydrous glucose rings of cellulose. Only one Methocel solution was used, since the flow behavior index was very close to unity (0.93-0.98) over the range of shear rates studies. The

ASSUMPTION UNIVERSITY LIBRARY

experimentally determined physical properties have been listed in Appendix IV, and further properties may be obtained from the Methocel handbook (18).

c) Carbose I.M. Carbose I.M. is a technical grade, medium viscosity type of sodium carboxy-methylcellulose manufactured by the Wyandotte Chemical Corporation. Two aqueous solutions of Carbose were employed, but one of the solutions (1%) did not conform to the power law model over the full shear rate range--this 1% by weight solution had a flow behavior index which increased with increasing shear rates. Further physical properties of Carbose may be obtained from the technical data sheet furnished by the Wyandotte Chemical Corporation and from the values listed in Appendix IV.

## CHAPTER VI

### RESULTS AND DISCUSSION

#### A. Physical Properties

##### Rheological Properties

All flow curve data for the non-Newtonian test fluids have been listed in Appendix IV. The experimental equipment, method and calibration data have been detailed previously in Chapter IV.

Figs. 2 and 3 were drawn to illustrate the variation of the "flow behavior index"  $N$  and "consistency index"  $K$  with temperature and also with percentage solids. In general, the flow behavior index decreased both for temperature increases and also as the percentage of dissolved solids was increased. The consistency index was found to increase with increasing temperature for the Carbopol systems but to decrease with increasing temperature for all other systems. The flow behavior index was found to remain constant over the full shear rate range covered except for the case of the 1% Carbose solution.

a) Carbopol 934. The strange behavior of the consistency index as a function of temperature for Carbopol was difficult to explain mainly because the exact formulation of the compound has not been revealed. One possible explanation lies in its manner of solution.



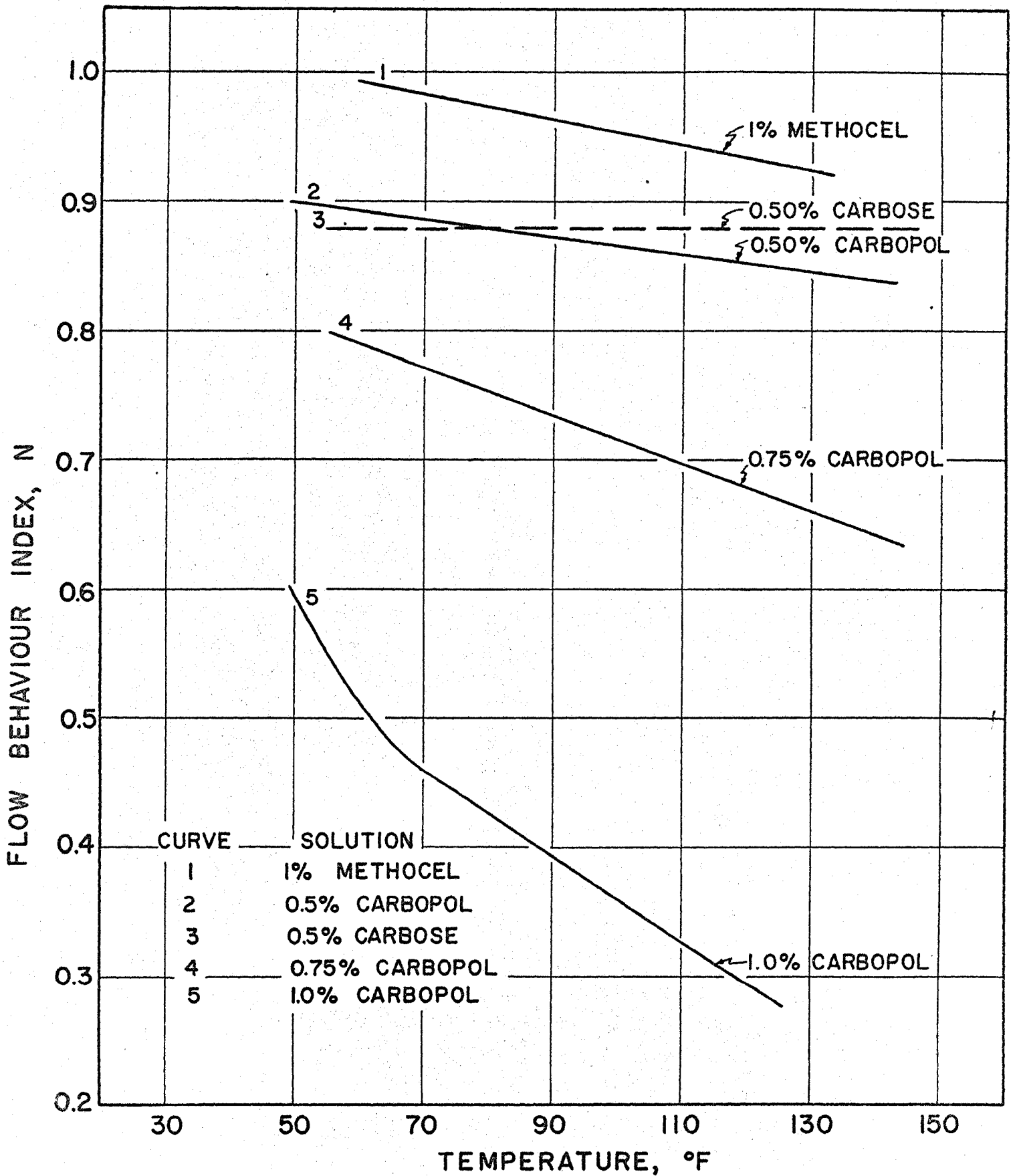


FIG. 2 FLOW BEHAVIOUR INDEX—AQUEOUS POLYMER SOLUTIONS

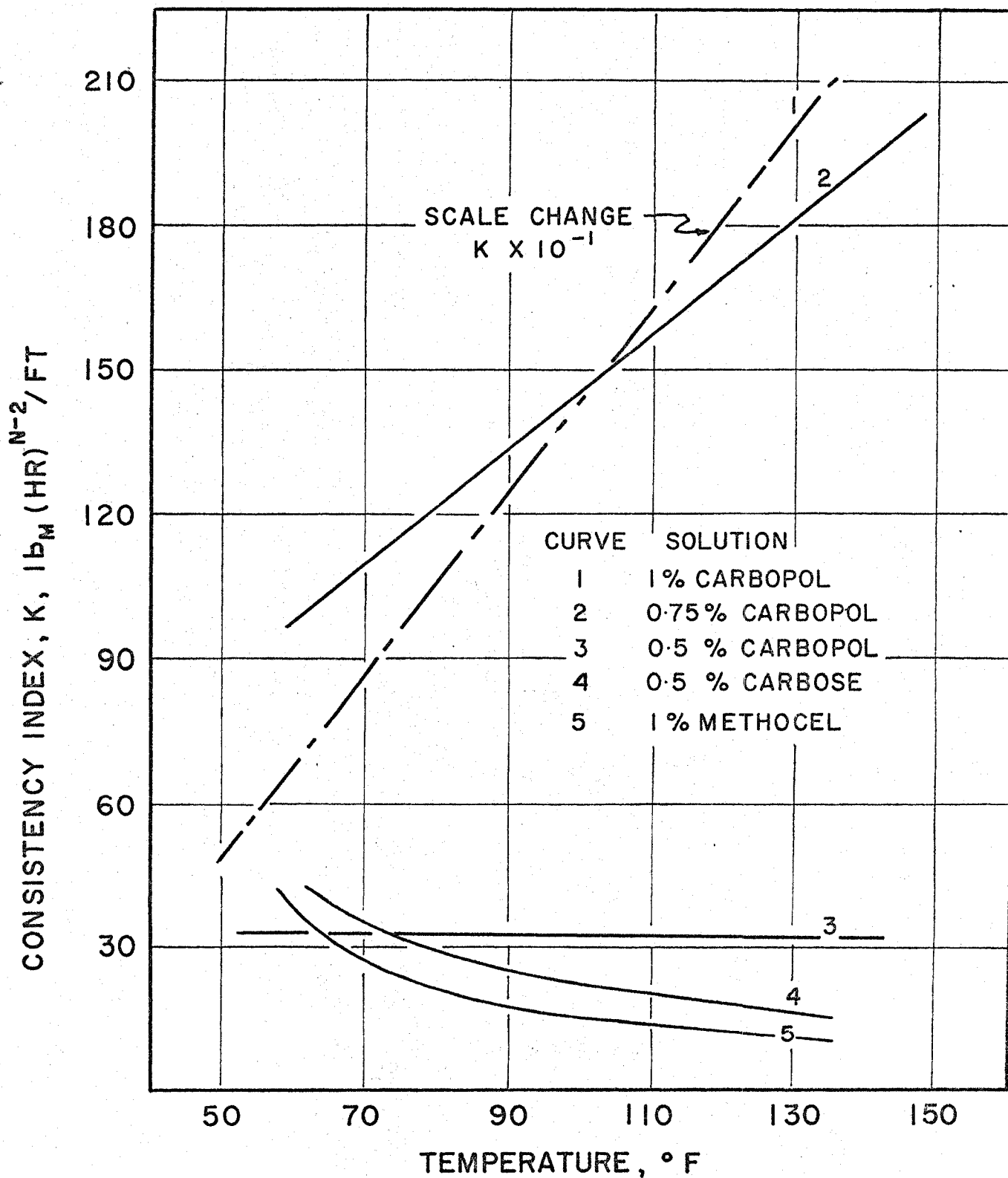


FIG. 3 CONSISTENCY INDEX—AQUEOUS POLYMER SOLUTIONS

Carbopol probably exists in solution as long threadlike molecules which are surrounded by successive layers of water which contribute to the bulk of the aggregate. As the temperature increases, the energy of these more or less loosely bound water molecules increases and those of the outer layers break away, causing the solubility of the Carbopol to decrease and the viscosity to increase since the lubricating water layers have been removed.

The manner of solution as postulated above would also explain the decreasing value of the flow index with increasing temperature since temperature increases would result in more Carbopol molecules coming out of solution--the net effect being an increase in the colloidal particle size of the Carbopol. For the Carbopol solutions,  $N$  ranged from 0.38-0.90.

b) 1% Methocel. The consistency index of the 1% Methocel solution was found to decrease with increasing temperature and the flow behavior index, which also decreased with increasing temperature, ranged from 0.92 at 135°F to 0.99 at 60°F. The value of  $N$  remained constant over the shear rate range studied.

The manner of solution of Methocel is similar to that described for Carbopol with the exception that the solubility is not so temperature sensitive. This allows the viscosity or consistency index to first decrease (due to decrease in viscosity of lubricating layers of water) and then to increase as the temperature is further increased, since the solubility effects become more predominant than the decreasing viscosity of the dispersing medium.

c) 0.5% Carbose. The behavior of the consistency index as a function of temperature was similar to that for the 1% Methocel solution, and the flow behavior index remained constant at 0.88 as the temperature varied from 60°F to 130°F. The flow behavior index was not a function of the shear rate over the range studied.

#### Thermal Conductivities

All the experimentally determined thermal conductivities have been listed in Appendix IV, and Fig. 4 gives the results in graphical form as a function of temperature. The experimental equipment, method and calibration data have been detailed previously in Chapter IV. The data obtained are in fair agreement with that obtained by Vaughn (29).

For all solutions the thermal conductivity increased with increasing temperature and as the weight percentage of dissolved solids was increased the thermal conductivity decreased. Table 2 details the results and gives a comparison with the thermal conductivity of water.

Table 2

Thermal Conductivities of Aqueous Polymer Solutions  
as Compared with Water

Solution	k 70°F Btu/hr.ft°F	% Difference from Water	k 130°F Btu/hr(ft)(°F)	% Difference from Water
1% Carbopol	0.307	- 11.5	0.330	- 12.0
0.75% Carbopol	0.318	- 8.4	0.348	- 7.2
0.50% Carbopol	0.327	- 5.8	0.358	- 4.5
1% Carbose	0.311	- 10.4	0.335	- 10.7
0.50% Carbose	0.326	- 6.0	0.359	- 4.3
1% Methocel	0.318	- 8.4	0.340	- 9.3

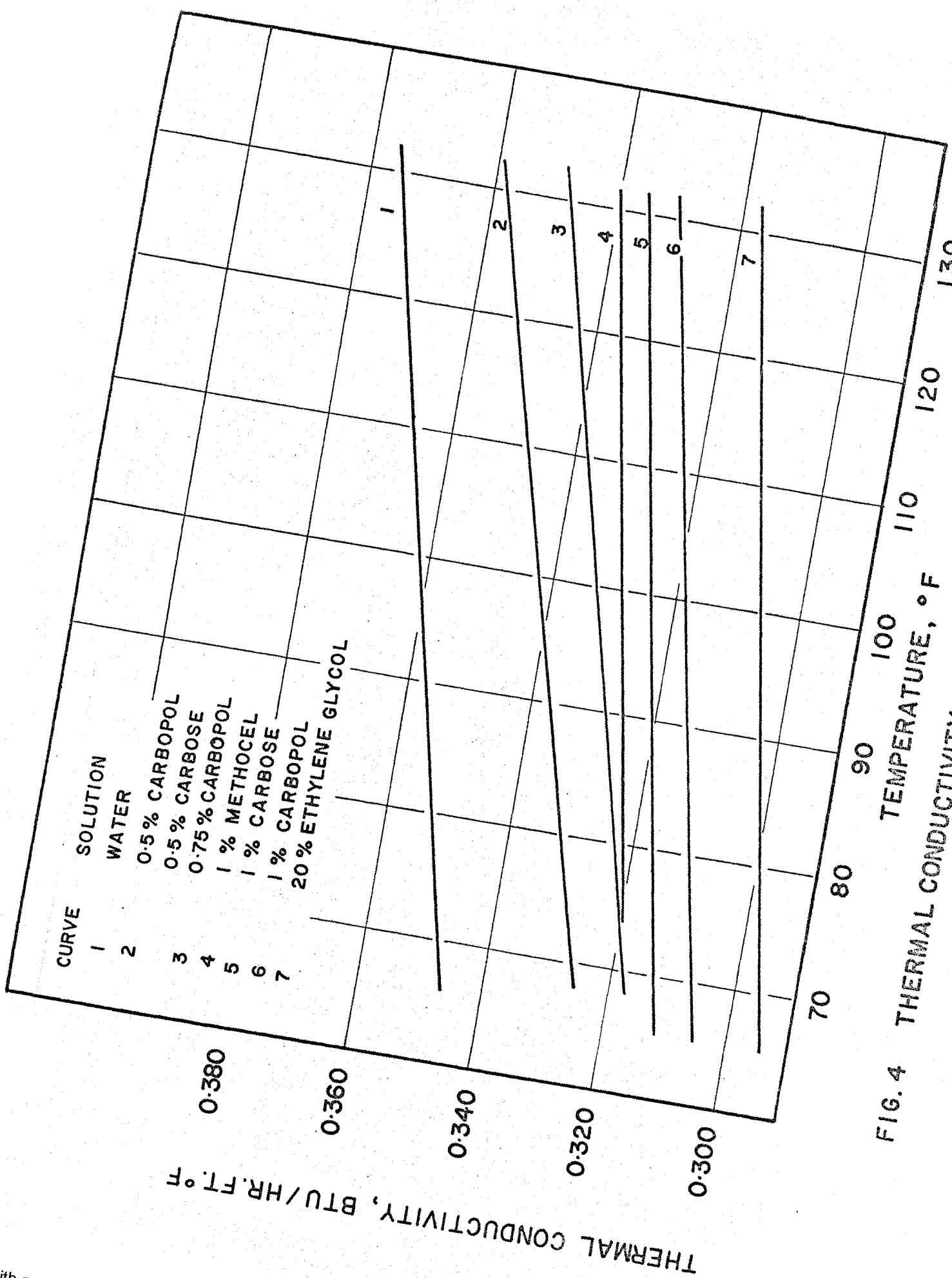


FIG. 4 THERMAL CONDUCTIVITY OF AQUEOUS POLYMER SOLUTIONS

THERMAL CONDUCTIVITY, BTU/HR.FT.°F

Reproduced with permission of the copyright owner. Further reproduction prohibited without permission.

## Densities and Coefficients of Thermal Expansion

The densities of all test solutions have been listed with the physical properties in Appendix IV, and the experimental apparatus, method and calibration data have been detailed previously in Chapter IV. The densities of all the aqueous polymer solutions were very slightly higher than that of water and the density increased as the percentage of dissolved solids was increased.

The calculated thermal expansion coefficients,  $\beta$ , are plotted in Fig. 5 as a function of temperature. They were very close to those for water, with the average percentage difference from water being  $\pm 3\%$ . For this reason the thermal expansion coefficients of water were used in all calculations of the dimensionless groups.

### B. Heat Transfer Results

All the heat transfer results and corresponding values of the dimensionless groups are listed in Appendix V. The following dimensionless groups used to correlate the results were obtained by dimensional analysis (Chapter III) employing the power law model:

$$N_{PR} = \frac{c_p \rho}{k} \left[ \frac{K}{e} \right]^{\frac{1}{2-N}} L^{\frac{2(N-1)}{N-2}} \quad (6.1)$$

$$N_{GR} = \frac{g \beta \Delta T L^{\frac{N+2}{2-N}}}{\left[ \frac{K}{e} \right]^{\frac{2}{2-N}}} \quad (6.2)$$

$$N_{Ra} = N_{PR} N_{GR} \quad (6.3)$$

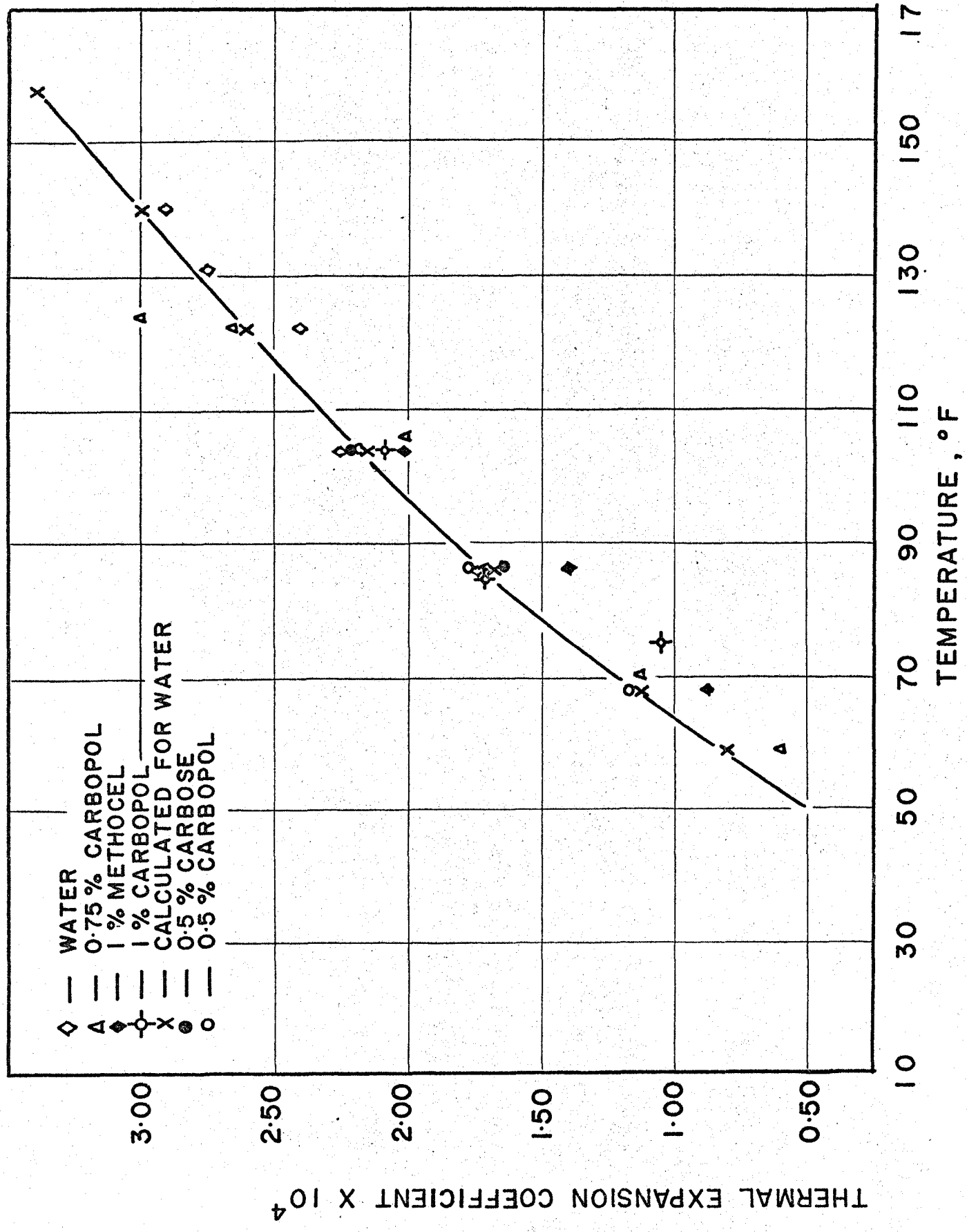


FIG.5 THERMAL EXPANSION COEFFICIENTS

In accordance with our dimensional analysis, it must be possible to describe the free convective heat transfer results by the equation:

$$N_{Nu} = A (N_{Ra})^a (N_{PR})^b (N)^c \quad (6.4)$$

where A, a, b and c are constants to be evaluated. The dimensionless groups used in determining these constants were all evaluated using physical properties at the arithmetic mean temperature of the two horizontal plates bounding the fluid.

The basic heat transfer data were plotted (Fig. 6) as a log-log plot of Nusselt number vs. Rayleigh number. The value of the exponent b ( $N_{PR}^b$ ) was assumed to be equal to 0.084, which was obtained by O'Toole and Silveston (22) from extensive data on several Newtonian fluids. The data were then replotted on log-log paper as  $N_{Nu} (N_{PR})^{-0.084}$  vs.  $N_{Ra}$  and by visual inspection the effect of N noted. From the graph of  $\log N_{Nu} (N_{PR})^{-0.084}$  vs. N with  $N_{Ra}$  as a parameter the first approximation of the value for the exponent c ( $N^c$ ) was calculated. Again the data were replotted (Fig. 7) on a log-log plot as  $N_{Nu} (N_{PR})^{-0.084} \left(\frac{N_{REF}}{N}\right)^{-c}$  vs.  $N_{Ra}$  which allowed a more accurate determination of the second approximation of c from the plot  $\log N_{Nu} (N_{PR})^{-0.084} \left(\frac{N_{REF}}{N}\right)^{-c}$  vs. N (Fig. 8). The final value of the constant c was found to be 1.75 and this value remained constant over the experimental Rayleigh range.



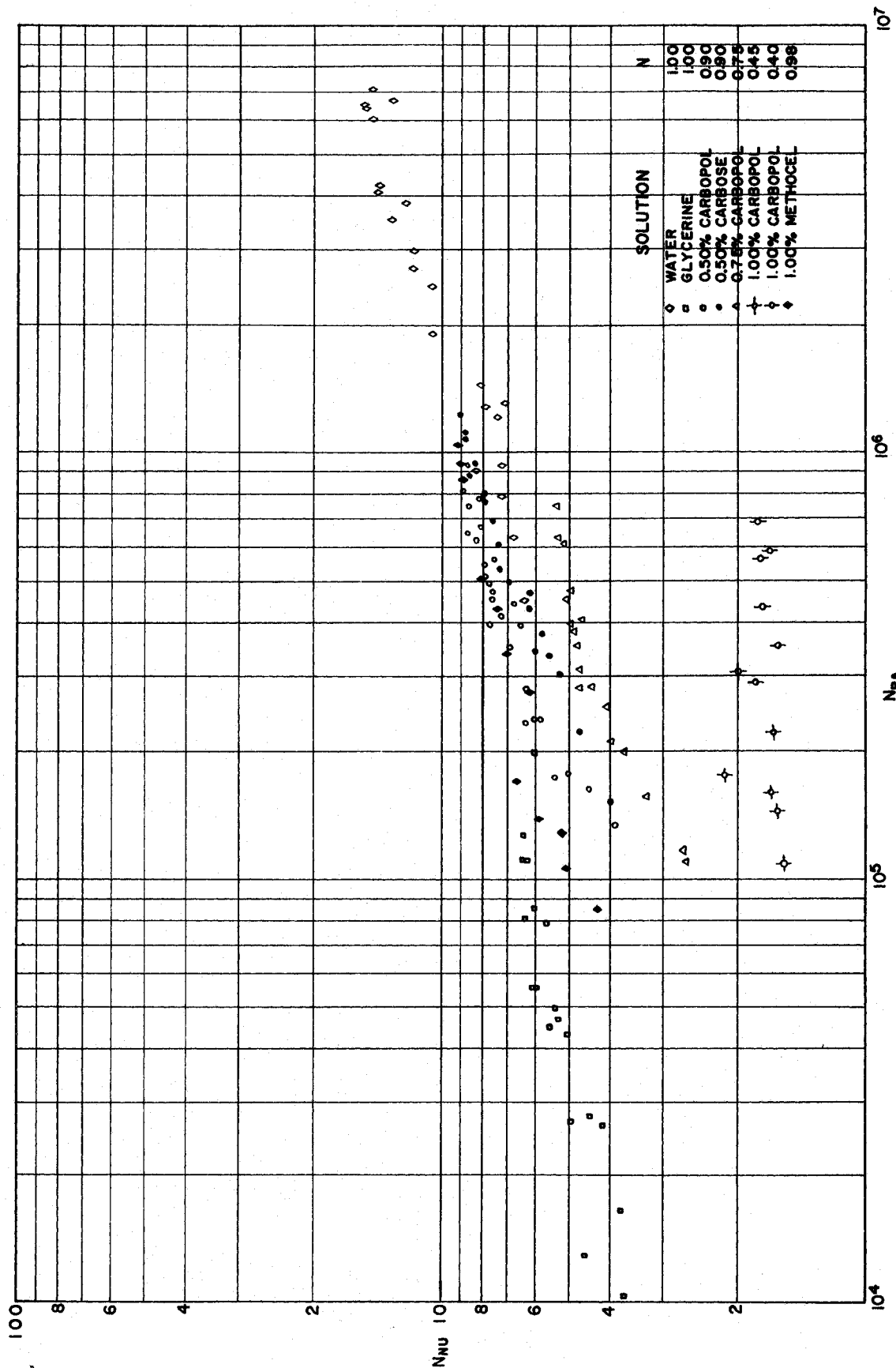


FIG. 6 EXPERIMENTAL DATA POINTS

ASSUMPTION UNIVERSITY LIBRARY

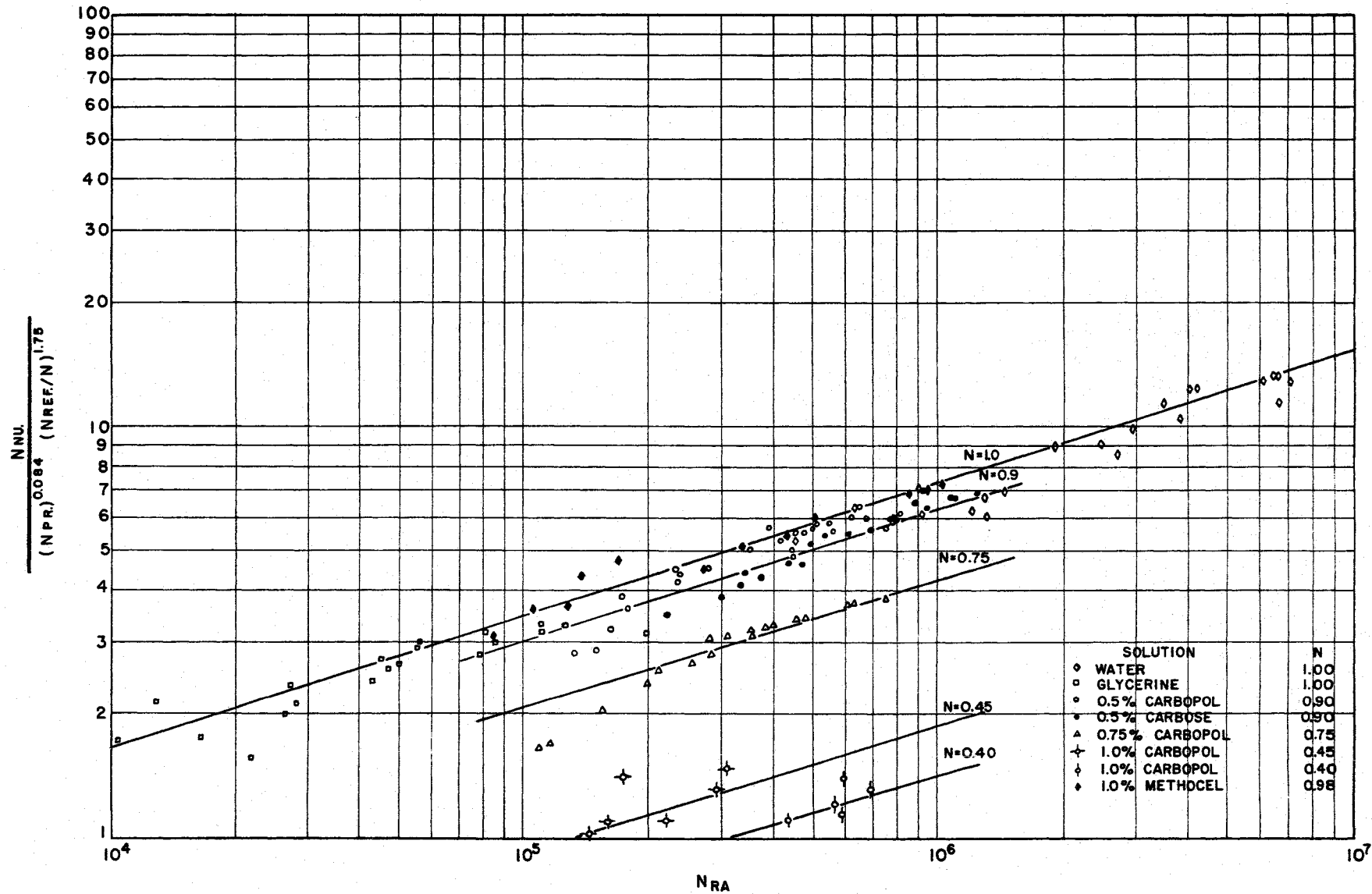


FIG-7 EXPERIMENTAL DATA CORRELATION

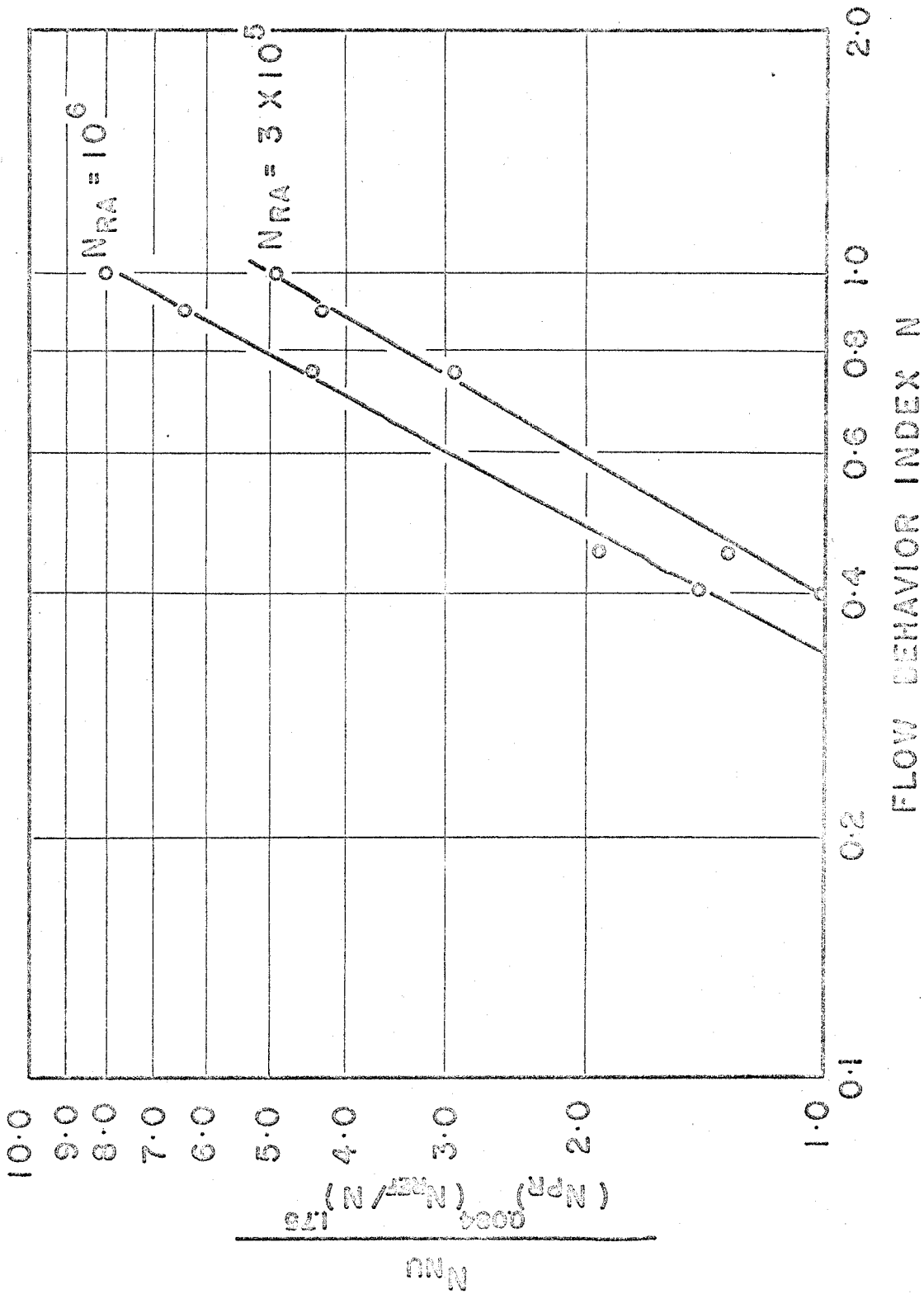


FIG.8 DETERMINATION OF EXPONENT C

The final experimental correlation was found from a plot of  $\log N_{Nu} (N_{PR})^{-0.084} N^{-1.75}$  vs.  $N_{Ra}$  and using the method of least squares the curve of best fit through the 130 experimental points was found. The equation obtained, which is believed to be valid for both Newtonian and non-Newtonian fluids is the following: (Fig. 9)

$$N_{Nu} = 0.0832 (N_{Ra})^{0.324} (N_{PR})^{0.084} (N)^{1.75} \quad (6.5)$$

$$\text{for } 0.38 < N < 1.00$$

$$10^4 < N_{Ra} < 10^7$$

$$4.45 < N_{PR} < 13.800$$

Equation (6.5) is in good agreement with the correlation of O'Toole and Silveston (22) for Newtonian fluids in the same Rayleigh number range. Table 3 summarizes the comparison of the correlations of this author and O'Toole's using calculated values of the Nusselt number.

Table 3

Comparison of Experimental Correlations

$N_{Ra}$	$N_{Nu}$ (O'Toole and Silveston)	$N_{Nu}$ (Author)	% Difference
10,000	2.33	1.66	-40.4
100,000	3.48	3.47	- 0.3
1,000,000	7.03	7.31	+ 3.8
10,000,000	14.2	15.4	+ 7.8

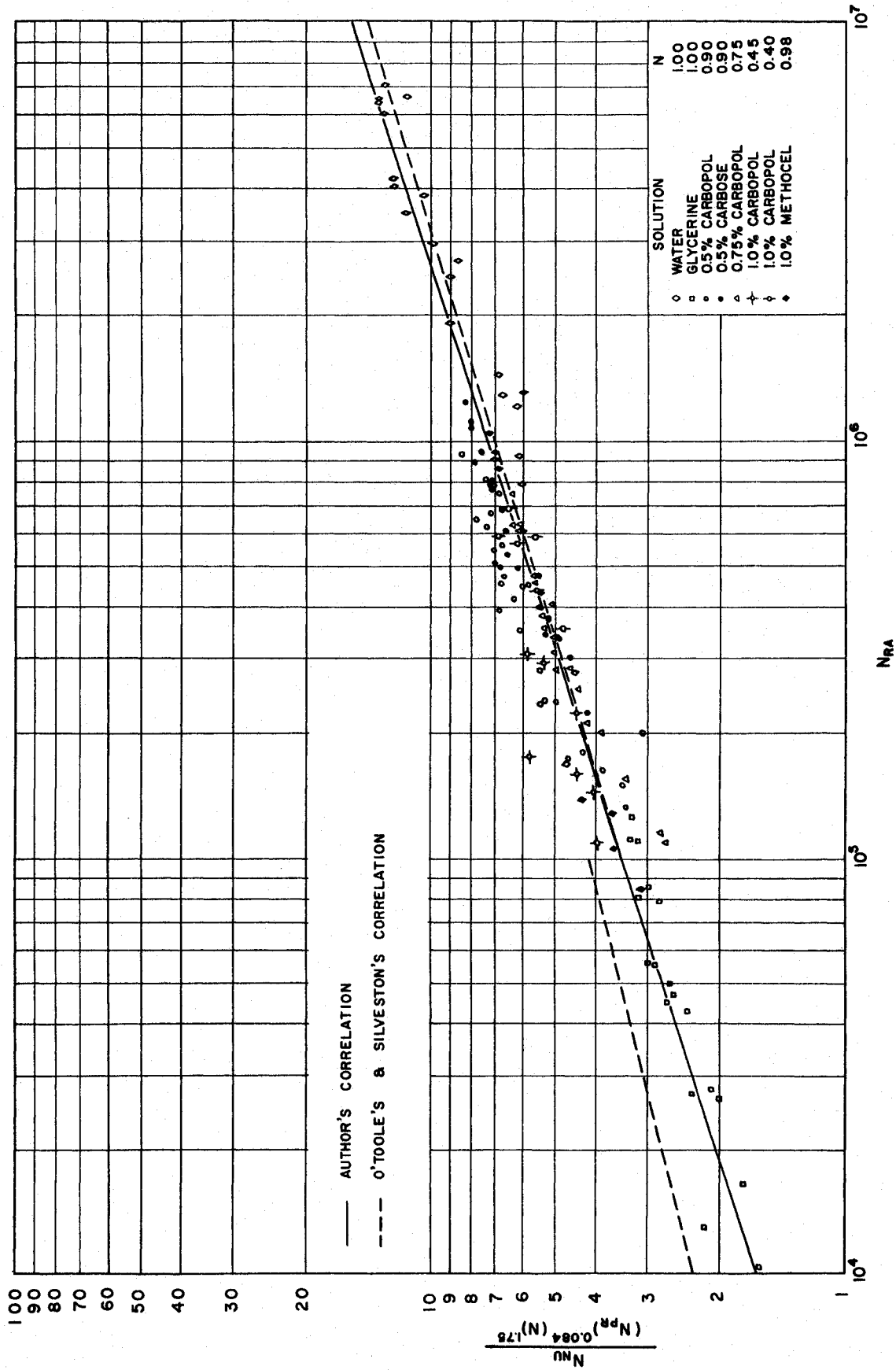


FIG. 9 FINAL EXPERIMENTAL DATA CORRELATION

In the preceding table it was shown that only in the lower Rayleigh number range ( $10^4$ ) is there any appreciable difference between the two correlations and this difference can be attributed to the following two causes:

- i) this author's data was correlated over two regions of flow: laminar and turbulent;
- ii) the correlation of O'Toole was based on two distinct regions of flow--turbulent where the Prandtl number has an effect and laminar where the Prandtl number was believed to have negligible effect.

Since the data obtained from glycerine for the laminar region, which for O'Toole's correlation corresponds to a Rayleigh's number ranging from 3500 to  $10^5$ , were found to be appreciably higher than O'Toole's correlation, the Prandtl number was believed to have an effect in this range. Due to the absence of more data in this range for fluids with relatively high Prandtl numbers, the effect of the Prandtl number was assumed to be the same as in the laminar region which led to satisfactory results.

From Fig. 7 the variation of the Nusselt number with the flow index,  $N$ , can be seen graphically. As  $N$  decreases, the  $N_{Nu}$  approaches to one and this would be the expected behavior since in the limit when  $N$  equals zero the shear rate becomes equal to zero (29) and the fluid is called an Euclid solid. However, the method employed here for correlating the results will give a value of zero for  $N_{Nu}$  when  $N$  equals zero and for this reason a correlation in the form of a log-log plot of  $(N_{Nu} - 1)$  vs.  $N_{Ra}$  could possibly have given results satisfying the limiting case.

From a theoretical viewpoint, the formulated generalized dimensionless groups and equation for natural convective heat transfer yielded a good correlation which indicates that the significant variables reasonably affecting the problem of natural convective heat transfer to non-Newtonian fluids have been taken into account.

## CHAPTER VII

### FUTURE RESEARCH

Based upon this study the following is a proposed list of future works of either theoretical or experimental nature which should yield useful information on free convective heat transfer to both Newtonian and non-Newtonian fluids:

- i) the effect of the Prandtl number in the so called laminar region be determined by obtaining extensive data in this region on more Newtonian fluids having high Prandtl numbers;
- ii) the range of dimensionless groups used in this study for non-Newtonian fluids be extended in order to obtain information on the convection point and applicability in the higher turbulent regime;
- iii) a theoretical study be made to determine the critical value of the dimensionless group for non-Newtonian fluids which would indicate the onset of convection;
- iv) for comparison with data on Newtonian fluids, optical observations be made on non-Newtonian fluids to determine the patterns formed in the layer by convection and to also determine the direction of circulation since the variation of viscosity (consistency) with temperature is the major effect determining the direction of circulation.



## NOMENCLATURE

a	= empirical exponent in equation (3.28), dimensionless
a <sup>+</sup>	= lumped parameter of physical properties,
	$\frac{g \beta \rho^2 C_p}{\mu K}, \text{ } ^\circ\text{F}^{-1}(\text{cu. ft.})^{-1}$
A	= empirical constant for thermal conductivity apparatus and empirical constant in equation (3.28)
b	= empirical exponent in equation (3.28), dimensionless
B	= empirical constant for thermal conductivity apparatus
c	= empirical exponent in equation (3.28), dimensionless
C <sub>p</sub>	= specific heat at constant pressure, Btu/lb. <sub>M</sub> °F
D	= diameter of bob for rotational viscometer, ft.
$(\frac{du}{dy}), (\frac{du}{dr})$	= shear rate, sec. <sup>-1</sup>
$(\frac{du}{dr})_i$	= shear rate at wall of bob for rotational viscometer, sec. <sup>-1</sup>
E	= voltage, volts
F <sub>1</sub>	= shearing stress at inside cylinder, $M/2\pi R_o^2 L_{eq}$ , lb. <sub>f</sub> /sq. ft.
$\vec{g}$	= gravitational force per unit mass, lb. <sub>f</sub> /lb. <sub>M</sub>
g <sub>c</sub>	= gravitational conversion factor, lb. <sub>M</sub> - ft/lb. <sub>f</sub> - sec <sup>2</sup>
G	= torque, ft. - lb. <sub>f</sub>
$\vec{G}$	= buoyancy force per unit volume, lb. <sub>f</sub> /cu. ft.
h	= heat transfer coefficient, Btu/hr. sq. ft. °F
I	= current, amps.
I.D.	= inside diameter of cylindrical fluid gap for heat transfer equipment, ft.
k	= thermal conductivity, Btu/hr. ft. °F
k <sub>1</sub> , k <sub>2</sub>	= instrument constants for rotational viscometer, dimensionless
K	= fluid consistency index, as defined by equation (3.4), lb. <sub>M</sub> /ft. (sec) <sup>2-N</sup> or lb. <sub>f</sub> (sec) <sup>N</sup> /sq. ft.

- L = characteristic dimension for length in dimensional analysis and fluid height in heat transfer apparatus, ft.
- $L_{eq}$  = equivalent bob length for rotational viscometer, ft.
- m = slope of logarithmic plot of shear rate vs. torque, dimensionless
- M = characteristic dimension for mass in dimensional analysis, lb.<sub>M</sub>
- n = flow behavior index as defined by equation (3.4), dimensionless
- $n_{REF}$  = flow behavior index used as reference in data correlation, dimensionless
- " = slope of logarithmic plot of torque vs. rotational speed, dimensionless
- $N_{GR}$  = Grashof number, taken as  $\frac{g \beta \Delta T L^3}{\nu^2}$  for Newtonian fluids, and as 
$$\frac{g \beta \Delta T L \frac{N+2}{2-N}}{\left[ \frac{K}{\rho} \right] \frac{2}{2-N}}$$
 for non-Newtonian fluids, dimensionless
- $N_{Nu}$  = Nusselt number, taken as  $\frac{hD}{k}$  for both Newtonian and non-Newtonian fluids, dimensionless
- $N_{PR}$  = Prandtl number, taken as  $\frac{c_p \mu}{K}$  for Newtonian fluids, and as 
$$\frac{c_p \mu}{k} \left[ \frac{K}{\rho} \right] \frac{1}{2-N} \cdot \frac{2(N-1)}{L \frac{2(N-1)}{N-2}}$$
 for non-Newtonian fluids, dimensionless
- $N_{Ra}$  = Rayleigh number  $N_{PR} \cdot N_{GR}$ , dimensionless
- q = heat flux, Btu/hr.sq.ft.
- Q = characteristic dimension for heat in dimensional analysis, Btu
- r = radius, ft;  $r_0$  and  $r_2$  denote radius of outer cylinder for rotational viscometer while  $r_1$  and  $r_i$  denote inside cylinder (bob) radius for rotational viscometer, ft.

R	= viscometer scale torque reading, zero to one, dimensionless
s	= radius ratio, $\frac{r_i}{r_o}$ , dimensionless
t	= temperature, °F
T	= torque, ft. lb. <sub>f</sub>
$\Delta T$	= temperature differential, °F
$v_s$	= specific volume, cu.ft./lb. <sub>M</sub>
W	= heat input, watts
x	= dimensionless exponent, equation (3.15)

## Greek Letters

$\alpha$	= thermal diffusivity, $\frac{k}{c_p \rho}$ , sq. ft./hr.
$\beta$	= coefficient of thermal expansion, $\frac{1}{v} \left( \frac{\partial v}{\partial T} \right)_p$ , °R <sup>-1</sup>
$\theta$	= temperature and characteristic dimension for temperature in dimensional analysis, °F
$\Delta \theta$	= temperature differential, °F
$\mu$	= viscosity of a Newtonian fluid, lb <sub>M</sub> /ft(sec) or lb <sub>M</sub> /ft.hr.
$\mu_A$	= apparent viscosity, $\tau / \left( \frac{du}{dy} \right)$ , lb. <sub>M</sub> /ft.sec.
$\nu$	= kinematic viscosity, sq.ft./sec.
$\pi$	= 3.1416
$\rho$	= fluid density, lb <sub>M</sub> /cu.ft.
$\tau$	= shear stress, $\tau_i$ and $\tau_o$ denote the shear stress at the inner and outer cylinders of the rotational viscometer respectively, lb. <sub>f</sub> /sq.ft.
$\tau_y$	= yield shear stress of a Bingham plastic, lb. <sub>f</sub> /sq.ft.
$\phi$	= apparent fluidity, $\frac{4\pi r_i^2 r_o^2 L \omega}{T(r_o^2 - r_i^2)}$ sq.ft./lb. <sub>f</sub> (sec)
$\omega$	= angular velocity rotational viscometer, rev/sec.

## LIST OF REFERENCES

1. Acrivos, Andreas, A.I.Ch.E. Journal, 6, 584 (1960).
2. Bénard, H., Rev. gen. sci., 11, 1261 (1900).
3. Bingham, E.C., Fluidity and Plasticity, McGraw-Hill Book Co., New York (1922).
4. De Graaf, J.G.A., and Van Der Held, E.F.M., Appl. Sci. Res., A3, 393 (1952).
5. Dodge, D.W. and Metzner, A.B., A.I.Ch.E. Journal, 5, 189 (1959).
6. Fredrickson, A.C., and Bird, R.B., Ind. Eng. Chem., 50, 347 (1958).
7. Globe, S., and Dropkin, D., A.S.M.E., Paper 21, Second Nat. Heat Transf. Conf., Chicago (1958).
8. Green, H., Industrial Rheology and Rheological Structures, John Wiley and Sons, New York (1949).
9. Jakob, M., Trans. Amer. Soc. Mech. Engrs., 68, 189 (1946).
10. Jeffreys, H., Proc. Roy. Soc. (London), A 118, 195 (1928).
11. Krieger, I.M., and Maron, S.H., J. Appl. Phys., 25, 72 (1954).
12. Krieger, I.M. and Elrod, H., J. Appl. Phys., 24, 134 (1953).
13. Krieger, I.M. and Maron, S.H., J. Appl. Phys., 23, 147 (1952).
14. Lange, N.A., Handbook of Chemistry, Handbook Pub. Inc., 9th ed. (1956).
15. Lord Rayleigh, Phil. Mag., 32, 29 (1916).
16. Low, A.R., Proc. Roy. Soc. (London), A125, 180 (1929).
17. Malkus, W.V.R., Proc. Roy. Soc. (London), A255, 185, 196 (1954).
18. Methocel, A Handbook of Data on Methocel, Dow Chem. Co. (1960)
19. Metzner, A.B., Advances in Chemical Engineering, Chapt. on Non-Newtonian Technology, Vol. I, Academic Press, New York (1956).
20. Mooney, M., Rheology, Frederick R. Eirich, ed., Vol. II, p. 207, Academic Press, New York (1958).

21. Mull, W., and Reiker, H., Beik. Z. Gesundheitstech.-Ing., Series I. 28 (1930).
22. O'Toole, J.L. and Silveston, P.L., Chem.Eng.Progr.Symp.Ser., No. 32, Vol. 57, Pg. 81 (1959).
23. Riedel, L., Mitt. Kaltetech. Inst. Tech. Hochschule, Karlsruhe (1948).
24. Schmidt, E. and Silveston, P.L., Chem.Eng.Progr.Symposium, Ser., No. 29, 55, 163 (1959)
25. Schmidt, R.J. and Milverton, S.W., Proc. Roy. Soc. (London), A152, 586 (1935).
26. Schmidt, R.J. and Saunders, O.A., Proc. Roy. Soc., A165, 216 (1938).
27. Stumpf, W., Diplomarbeit, Technische Hochschule Muenchen, Munich, Germany (1957).
28. Thompson, J., Proc. Glasg. Phil. Soc., 13, 464 (1882).
29. Vaughn, R.D., Ph.D. Thesis, Heat Transfer to Non-Newtonian Fluids, University of Delaware (1956).
30. Wilkinson, W.L., Non-Newtonian Fluids, London, Pergamon Press (1960).

APPENDIX I

NEWTONIAN FLUIDS IN NATURAL CONVECTION

## APPENDIX I

### NEWTONIAN FLUIDS IN NATURAL CONVECTION

The quantities which we can reasonably expect to affect the problem of free convection are the following:

<u>Quantity</u>	<u>Symbol</u>	<u>Dimensions</u>	
Length	L	ft.	[L]
Buoyant Acceleration	$g\beta$	ft/sec <sup>2</sup> (°F)	[L T <sup>-2</sup> θ <sup>-1</sup> ]
Density	$\rho$	lb. <sub>M</sub> /ft <sup>3</sup>	[M L <sup>-3</sup> ]
Viscosity	$\mu$	lb. <sub>M</sub> /ft.sec.	[M L <sup>-1</sup> T <sup>-1</sup> ]
Thermal Conductivity	k	Btu/ft(sec)°F	[Q L <sup>-1</sup> T <sup>-1</sup> θ <sup>-1</sup> ]
Temperature Difference	$\Delta \theta$	°F	[θ]
Specific Heat	$c_p$	Btu/lb. <sub>M</sub> °F	[Q M <sup>-1</sup> θ <sup>-1</sup> ]
Heat Transfer Coefficient	h	Btu/ft <sup>2</sup> (sec)°F	[Q L <sup>-2</sup> T <sup>-1</sup> θ <sup>-1</sup> ]

The solution of our problem should contain dimensionless parameters in the form of products of powers of the various variables involved. Each of the parameters must be of the form

$$L^{x_1} (g\beta)^{x_2} \rho^{x_3} \mu^{x_4} k^{x_5} \Delta \theta^{x_6} c_p^{x_7} h^{x_8}$$

where  $x_1, x_2, \dots, x_8$  denote exponents which are unknown this far.

Writing down the dimensions of the above product, we obtain:

$$[L]^{x_1} [L T^{-2} \theta^{-1}]^{x_2} [M L^{-3}]^{x_3} [M L^{-1} T^{-2}]^{x_4} \\ [Q L^{-1} T^{-1} \theta^{-1}]^{x_5} [\theta]^{x_6} [Q M^{-1} \theta^{-1}]^{x_7} [Q L^{-2} T^{-1} \theta^{-1}]^{x_8}$$

In order for the above product to be dimensionless, we can equate the dimensions of time, mass, heat, length and temperature respectively to zero and obtain five equations for the eight unknown exponents.

For the dimension of length [L]

$$(1) \quad x_1 + x_2 - 3x_3 - x_4 - x_5 - 2x_8 = 0$$

For the dimension of time [T]

$$(2) \quad -2x_2 - x_4 - x_5 - x_8 = 0$$

For the dimension of temperature [ $\theta$ ]

$$(3) \quad -x_2 - x_5 + x_6 - x_7 - x_8 = 0$$

For the dimension of heat [Q]

$$(4) \quad x_3 + x_7 + x_8 = 0$$

For the dimension of mass [M]

$$(5) \quad x_3 + x_4 - x_7 = 0$$

We now have three exponents which are indeterminate and may be chosen arbitrarily; the remaining five exponents being expressed in terms of the chosen three. When  $x_6$ ,  $x_7$  and  $x_8$  are arbitrarily chosen and  $x_1$ ,  $x_2$  ...  $x_8$  expressed in terms of them, we find that:



$$x_1 = 3x_6 + x_8$$

$$x_2 = x_6$$

$$x_3 = 2x_6$$

$$x_4 = -2x_6 + x_7$$

$$x_5 = -x_7 - x_8$$

This results in the following power product:

$$L^{3x_6+x_8} (g\beta)^{x_6} \rho^{2x_6} \mu^{-2x_6+x_7} k^{-x_7-x_8} \Delta\theta^{x_6} c_p^{x_7} h^{x_8}$$

The three arbitrary exponents may be disposed of by setting each in turn equal to one while simultaneously setting the remaining two equal to zero.

Thus, for  $x_6 = 1; x_7 = x_8 = 0$

$$\frac{L^3 g \beta \rho^2 \Delta\theta}{\mu^2} = \frac{L^3 g \beta \Delta\theta}{\nu^2} = N_{GR}$$

For  $x_7 = 1; x_6 = x_8 = 0$

$$\frac{\mu c_p}{k} = \frac{\mu/e}{k/c_p e} = \frac{\nu}{\alpha} = N_{PR}$$

Finally, for  $x_8 = 1, x_6 = x_7 = 0$

$$\frac{h L}{k} = N_{Nu}$$

The required function thus contains three dimensionless arguments and has one of the now familiar forms:

$$N_{Nu} = f(N_{GR}, N_{PR})$$

$$\text{or } N_{Nu} = C N_{Ra}^m N_{PR}^n$$

The constant  $C$  and exponents  $m$  and  $n$  must be determined from experimental results.

#### CREEPING MOTION IN FREE CONVECTION

For creeping motion, the inertia forces become negligible and the inertia forces arising in a medium are determined by the density of the medium. In the energy equation, the density is coupled with the specific heat  $c_p$  and if we introduce the specific heat per unit volume  $C_p = c_p \rho$ , the density no longer appears explicitly. We cannot simply neglect the density as being one of our variables since it has particular importance on the body force which is of great importance in natural convection.

Thus, the quantities which we can reasonably expect to affect creeping motion in free convection are the following:

<u>Quantity</u>	<u>Symbol</u>	<u>Dimensions</u>
Length	$L$	$[L]$
Viscosity	$\mu$	$[M L^{-1} T^{-1}]$
Specific heat per unit volume	$C_p = c_p \rho$	$[QL^{-3} \theta^{-1}]$
Thermal conductivity	$k$	$[QL^{-1} T^{-1} \theta^{-1}]$
Temperature difference	$\Delta \theta$	$[\theta]$
Buoyant force per unit volume	$g \beta \rho$	$[ML^{-2} T^{-2} \theta^{-1}]$
Heat transfer coefficient	$h$	$[QL^{-2} T^{-1} \theta^{-1}]$

The dimensionless parameters must be of the form

$$L^{x_1} \mu^{x_2} C_p^{x_3} k^{x_4} \Delta \theta^{x_5} (g \beta \rho)^{x_6} h^{x_7}$$

where  $x_1, x_2 \dots x_N$  denote the unknown exponents. Writing down the

dimensions of the above product we obtain:

$$[L]^{x_1} [M L^{-1} T^{-1}]^{x_2} [Q L^{-3} \theta^{-1}]^{x_3} [Q L^{-1} T^{-1} \theta^{-1}]^{x_4} \\ [\theta]^{x_5} [M K^{-2} T^{-2} \theta^{-1}]^{x_6} [Q L^{-2} T^{-1} \theta^{-1}]^{x_7}$$

In order for the above product to be dimensionless, we can equate the dimensions of time, mass, heat, length and temperature respectively to zero and obtain five equations for the seven unknowns.

For the dimension of length [L]

$$(1) \quad x_1 - x_2 - 3x_3 - x_4 - 2x_6 - 2x_7 = 0$$

For the dimension of time [T]

$$(2) \quad -x_2 - x_4 - 2x_6 - x_7 = 0$$

For the dimension of temperature [ $\theta$ ]

$$(3) \quad -x_3 - x_4 + x_5 - x_6 - x_7 = 0$$

For the dimension of heat [Q]

$$(4) \quad x_3 + x_4 + x_7 = 0$$

For the dimension of mass [M]

$$(5) \quad x_2 + x_6 = 0$$

We now have two exponents which are indeterminate and may be chosen arbitrarily; the remaining five exponents being expressed in

terms of two chosen arbitrarily. When  $x_6$  and  $x_7$  are arbitrarily chosen and  $x_1, x_2 \dots x_5$  expressed in terms of them we find that:

$$x_1 = 3x_6 + 1x_7$$

$$x_2 = + x_6$$

$$x_3 = x_6$$

$$x_4 = -x_6 - x_7$$

$$x_5 = x_6$$

This results in the following power product:

$$L^{3x_6 + 1x_7} \mu^{-x_6} C_p^{x_6} k^{-x_6 - x_7} (\Delta \theta)^{x_6} (g\beta e)^{x_6} h^{x_7}$$

Setting  $x_6 = 1$  and  $x_7 = 0$ , we obtain

$$\frac{L^3 C_p \Delta \theta (g\beta e)}{\mu k} = \frac{L^3 g \beta \Delta \theta}{\nu^2} \frac{\nu C_p e}{k} = N_{GR} N_{PR}$$

$$= N_{Ra}$$

For  $x_7 = 1$  and  $x_6 = 0$ , we obtain

$$\frac{h L}{k} = N_{Nu}$$

Thus for very slow or creeping motion in free convection, we obtain

$$N_{Nu} = f(N_{GR} N_{PR}) = f(N_{Ra})$$

$$\text{or } N_{Nu} = C N_{Ra}^n$$

where the constant  $C$  and exponent  $n$  are obtained from experimental results.

APPENDIX II  
CALIBRATION DATA

## APPENDIX II

### CALIBRATION OF ROTATIONAL VISCOMETER

The Brookfield Synchro-Lectric Viscometer was calibrated to correct for the small end effect using National Bureau of Standards Viscometer Calibrating Liquids (Oil Type K and M).

#### Calibration of Brookfield U. L. Adapter

For concentric cylinder viscometers

$$\frac{\mu}{g} = \frac{G (r_2^2 - r_1^2)}{4\pi r_1^2 r_2^2 L} = \frac{[1 - (r_1/r_2)^2] G}{4\pi L r_1^2 \omega}$$

or the equivalent length is given by

$$L_{eq} = \frac{[1 - (r_1/r_2)^2] g G}{\mu 4\pi r_1^2 \omega}$$

where:

$G$	:	=	$4.969 \times 10^{-5}$ R ft. - lb. <sub>f</sub>
$R$	:	=	viscometer torque scale reading (0 - 1)
$r_1$	:	=	inside radius = 0.0413 ft.
$r_2$	:	=	outside radius = 0.0452 ft.
$r_1/r_2$	:	=	0.914
$g$	:	=	$32.17 \text{ lb}_M / \text{lb}_f \text{ ft/sec}^2$
$\omega$	:	=	$2\pi N$ (where N is rps)
$\mu$	:	=	viscosity of calibrating oil

Substituting in the above quantities and using N.B.S. Oil K,  
Lot No. 17 for 25 C:

$$L_{eq} = 0.876 \times \frac{R}{N}$$

where N = rps

$L_{eq}$  = equivalent length in feet

or  $L_{eq} = 63.2 R/N$

where N = rpm

$L_{eq}$  = equivalent length in inches

Table 4  
Viscometer Flow Data

(for Oil K, Lot No. 17; T = 25 °C; $\mu = 0.3311$ poise)		
R. P. M.	R x 10 <sup>2</sup>	$L_{eq}$ (in)
3	17.2	3.62
6	34.3	3.61
12	68.6	3.61
(for Oil K at 100 F; $\mu = 0.1836$ poise)		
6	19.3	3.65
12	38.4	3.64
30	95.1	3.61
(for Oil M, Lot No. 31; T = 25 C; $\mu = 2.447$ poise)		
0.6	25.4	3.62
1.5	63.0	3.59
(for Oil M, Lot No. 31; T = 100 F; $\mu = 1.094$ poise)		
0.6	11.9	3.64
1.5	28.6	3.64
3	57.1	3.64

Equivalent length of inner cylinder equals 3.62 inches.

Actual length of inner cylinder equals 3.573 inches.

Calibration of Spindle No. 1

--Brookfield Synchro-Electric Viscometer--

Again, for concentric rotational viscometers:

$$\mu = \frac{[1 - (r_1/r_2)^2] G g}{4\pi L r_1^2 \omega}$$

and

$$L_{eq} = \frac{[1 - (r_1/r_2)^2] G g}{4\pi r_1^2 \omega \mu}$$

where

$$G = 4.969 \times 10^{-5} (R) \text{ ft.} - \text{lb.}_f$$

$$r_1 = 0.03096 \text{ ft.}$$

$$r_2 = 0.125 \text{ ft.}$$

$$\omega = 2\pi N$$

$$S = \text{torque scale reading (0 - 1)}$$

$$N = \text{rps}$$

$$L_{eq} = 87.1 \frac{S}{N} \text{ (inches)}$$

for N.B.S. Oil Type M at 25.0 C with  $\mu = 2.447$  poise and  $N = \text{rpm}$ .

$$L_{eq} = 3.01 \text{ inches}$$

Actual length of spindle No. 1 equals 2.56 inches.



Table 5  
Viscometer Flow Data

R. P. M.	$R \times 10^2$	$L_{eq}$ (in)
N.B.S. Oil M, $T = 25.0^\circ\text{C}$ ; $\mu = 2.447$ poise		
1.5	5.2	3.02
3	10.2	2.96
6	20.4	2.96
12	40.7	2.95
N.B.S. Oil M; $T = 100^\circ\text{F}$ ; $\mu = 1.094$ poise		
3	4.7	3.06
6	9.4	3.06
12	18.9	3.07
30	47.1	3.06
60	94.2	3.06
N.B.S. Oil K; $T = 20.0^\circ\text{C}$ ; $\mu = 0.4313$ poise		
3	1.8	2.96
6	3.7	3.05
12	7.2	2.96
30	17.8	2.93
60	35.9	2.96
N.B.S. Oil K; $T = 25.0^\circ\text{C}$ ; $\mu = 0.3311$ poise		
3	1.4	3.00
6	2.8	3.00
12	5.6	3.00
30	14.2	3.05
60	28.4	3.05

### CALIBRATION OF THERMAL CONDUCTIVITY APPARATUS

Redistilled water and a 20% ethylene glycol solution were used for calibration and determination of the apparatus constants A and B. The following tables summarize the calibration data.

Table 6

Thermal Conductivity Calibration Data--Water

EI = W Watts	$\Delta T$ °C	$EI/T$ <sup><math>\Delta T</math></sup> Watts/°C	T °C
0.7292	1.33	0.5483	32.05
0.8685	1.60	0.5428	33.17
0.8891	1.67	0.5323	36.10
0.9581	1.76	0.5471	48.03
0.96657	1.77	0.5461	55.32
0.96657	1.78	0.5430	58.09

Table 7

Thermal Conductivity Calibration Data--20% Ethylene Glycol

EI = W Watts	$\Delta T$ °C	$EI/T$ <sup><math>\Delta T</math></sup> Watts/°C	T °C
0.7064	1.71	0.4131	31.11
1.2252	2.75	0.4455	36.33
1.0224	2.58	0.3963	38.73
1.0248	2.46	0.4166	45.73

Table 8

## Thermal Conductivity Apparatus Constants

$$\frac{W}{\Delta T} = A k_M + B$$

T °C	Water		20% Ethylene Glycol			
	W/ΔT Watts/°C	k Btu/hr.ft. °C	W/ΔT Watts/°C	k Btu/hr.ft.°F	A	B
20	0.5475	0.344	0.4120	0.300	2.793-0.413	
40	0.5460	0.360	0.4120	0.308	2.552-0.373	
60	0.5450	0.375	0.4120	0.320	2.418-0.362	

APPENDIX III

DIRECT DETERMINATION OF THE FLOW CURVE OF NON-NEWTONIAN FLUIDS

### APPENDIX III

#### DIRECT DETERMINATION OF THE FLOW CURVE OF NON-NEWTONIAN FLUIDS

The method of Krieger and Elrod (12) developed for obtaining the flow curves of non-Newtonian fluids from concentric cylinder viscometer data was developed for the case in which the outer cylinder or cup rotates and the inner cylinder or bob is stationary. However, for our case the bob rotated and the outer cylinder remained stationary. Thus the following treatment was made to see if this method of Krieger and Elrod (12) was applicable for our case:

Unlike Newtonian fluids whose viscosity coefficients are constant, many colloidal suspensions and macromolecular solutions exhibit variation of viscosity with rate of shear. The flow behavior of these non-Newtonian fluids can be defined by the rheological equation

$$\left( - \frac{du}{dy} \right) = g(\mathcal{T}) \quad (1)$$

where  $(-du/dy)$  is again the rate of shear and  $\mathcal{T}$  is the shearing stress.

The above equation of flow must be integrated in order to obtain relationships among the experimental variables measured in viscometers. If the function  $g(\mathcal{T})$  is known this integration can be readily performed, but if it is desired to determine  $g(\mathcal{T})$  from experimental variables, then it becomes necessary to solve an integral equation.

Consider a concentric cylinder viscometer having an inner cylinder or bob of length  $L$  and radius  $r_i$  and an outer cylinder of

radius  $r_0$ . The inner cylinder rotates with constant angular velocity ( $\omega_i$ ) due to an external torque ( $T$ ). For laminar flow in the annular gap between the inner and outer cylinders, the rate of shear at a distance  $r$  from the axis where the fluid has angular velocity  $\omega$  is given by:

$$g(\tau) = r \left( - \frac{d\omega}{dr} \right) = \left( - \frac{d\omega}{d \ln r} \right) \quad (2)$$

The shearing stress is

$$\tau = \frac{T}{2\pi L} \frac{1}{r^2} \quad (3)$$

For constant or steady flow conditions,  $T$  is constant and from eq. (3)

$$r^2 = \frac{T}{2\pi L \tau}$$

and

$$2r dr = \frac{T}{2\pi L} \left[ - \frac{d\tau}{\tau^2} \right]$$

or

$$\frac{dr}{r} = - \frac{1}{2} \left[ \frac{d\tau}{\tau} \right] = \frac{T}{4\pi r^2 L} \left[ - \frac{d\tau}{\tau^2} \right]$$

or

$$d \ln \tau = - 2 d \ln r \quad (4)$$

and

$$g(\tau) = + 2 \left( \frac{d\omega}{d \ln \tau} \right)$$

or

$$d\omega = + \frac{1}{2} \frac{g(\tau) d\tau}{\tau} \quad (5)$$

Equation (5) can be integrated between the limits  $\tau = \tau_1$ ,  $\omega = \omega_i$  at the bob, and  $\tau = \tau_0$ ,  $\omega_0 = 0$  at the stationary cylinder.

Integrating between these limits, the following is obtained:

$$\int_{w_i}^0 dw = + \frac{1}{2} \int_{\tau_i}^0 \frac{g(\tau)}{\tau} d\tau$$

or

$$w_i = - \frac{1}{2} \int_{\tau_i}^0 \frac{g(\tau)}{\tau} d\tau \quad (6)$$

However, since

$$\frac{\tau_i}{\tau_0} = \frac{r_0^2}{r_1^2} = s^2$$

then

$$\tau_i = \tau_0 s^2 \quad (7)$$

Substituting eq. (7) into eq. (6) we obtain:

$$w_i = - \frac{1}{2} \int_{\tau_i}^{\tau_i s^{-2}} \frac{g(\tau)}{\tau} d\tau \quad (8)$$

Differentiating eq. (8) with respect to  $\tau_i$ , a difference equation is obtained:

$$\frac{dw_i}{d\tau_i} = - \frac{1}{2} \left[ \frac{g(\tau_i s^{-2})}{\tau_i s^{-2}} s^{-2} - \frac{g(\tau_i)}{\tau_i} \right]$$

or

$$\frac{dw_i}{d\tau_i} = - \frac{1}{2} \tau_i [g(\tau_0) - g(\tau_i)]$$

$$\frac{dw_i}{d\tau_i} = + \frac{1}{2} \tau_i [g(\tau_i) - g(\tau_0)] \quad (9)$$

This is the same difference equation as obtained by Krieger and Elrod (12) and the solution of the difference equation is applicable to our case. Thus, the single bob method developed by Krieger and Maron (11) based upon the solution of this difference equation (12) was used in the determination of all flow curves for the non-Newtonian fluids.



APPENDIX IV  
PHYSICAL PROPERTIES OF TEST FLUIDS

APPENDIX IV

Table 9

Physical Properties of Water

$t$ °F	$\rho$ lb <sub>M</sub> /ft <sup>3</sup>	$\mu$ lb <sub>M</sub> /hr.ft.	$k$ Btu/hr.ft. °F	$c_p$ Btu/lb <sub>M</sub> °F	$N$ PR	$a^+ \times 10^{-6}$ ft <sup>-3</sup> °F <sup>-1</sup>	$t$ °F	$\beta$ °R <sup>-1</sup> $\times 10^4$
40	62.43	3.74	0.326	1.0041	11.5	...		
50	62.41	3.16	0.334	1.0013	9.49	53.7	50.0	0.48
60	62.36	2.72	0.341	0.99996	7.98	154	59.0	0.82
70	62.30	2.37	0.347	0.9987	6.81	238	68	1.13
80	62.22	2.08	0.353	0.9982	5.89	330	86	1.69
90	62.12	1.85	0.358	0.9980	5.15	435		
100	62.00	1.65	0.363	0.9980	4.55	547	104	2.15
110	61.86	1.49	0.367	0.9982	4.06	670	122	2.60
120	61.71	1.35	0.371	0.9985	3.64	804		
130	61.55	1.24	0.375	0.9989	3.29	949	140	3.00
140	61.38	1.13	0.378	0.9994	3.00	1100		
150	61.20	1.05	0.381	1.000	2.74	1270	158	3.39

References:

- (1) Heat Transfer; B. Gebhart, McGraw-Hill Publ.Co.; 1961,
- (2) Handbook of Chemistry, Lange, 9th ed., Handbook Publishers, Inc., 1956.

$$a^+ = \frac{g \beta \rho^2 c_p}{\mu K}$$

Table 10  
Physical Properties of Glycerine

$t_F$	$\rho$ lb <sub>M</sub> /ft <sup>3</sup>	$c_p$ Btu/lb <sub>M</sub> °F	$\nu$ ft <sup>2</sup> /sec.	$\mu$ lb <sub>M</sub> /hr.ft.	$k$ Btu/hr.ft	$N_{PR}$ x10 <sup>-3</sup>	$\beta_{R-1}$ x10 <sup>+3</sup>	$a^+$ x10 <sup>-5</sup>
32	79.66	0.540	0.0895	25.7	0.163	84.7		
40	79.50	0.546			0.163		0.24	
50	79.29	0.554	0.0323	9.22	0.164	31.0	0.24	2.30
60	79.08	0.563		5.20	0.164	17.8	0.25	4.30
68	78.91	0.570	0.0127	3.61	0.165	12.5	0.28	6.97
80	78.66	0.580		1.98	0.165	6.96	0.28	12.8
86	78.54	0.584	0.0054	1.53	0.165	5.38	0.29	17.3
90	78.45	0.589		1.28	0.165	4.56	0.30	21.4
104	78.16	0.600	0.0024	0.675	0.165	2.45	0.35	48.0
110	78.03	0.605		0.580	0.1655	2.12	0.38	61.0
122	77.72	0.617	0.0016	0.448	0.166	1.63		92.2

$$a^+ = \frac{g \beta \rho^2 c_p}{\mu k}$$

## Sources:

- (1) Heat and Mass Transfer, Eckert, E.R.G. and Drake, R.M.Jr.; McGraw-Hill Bk.Co., Inc., 1959.
- (2) Handbook of Chemistry, Lange, 9th ed., Handbook Publishers Inc., 1956.

Table 11  
Physical Properties of Carbopol

$t$ $^{\circ}\text{F}$	$\rho$ $\text{lb}_M/\text{ft}^3$	$k$ $\text{Btu}/\text{hr}.\text{ft}.\text{ }^{\circ}\text{F}$	$n$ Flow Index	$c_p$ $\text{Btu}/\text{lb}_M(\text{ }^{\circ}\text{F})$	$\beta$ $^{\circ}\text{R}^{-1}$ $\times 10^4$	$K$ $\text{lb}_M/\text{ft} (\text{hr})^{2-N}$
(0.5% sol'n by weight; pH = 3.0)						
57.2	62.48	0.320	0.90	1.0	0.75	32.4
68.4	62.42	0.326	0.89	1.0	1.21	32.4
86.0	62.26	0.335	0.88	1.0	1.64	32.4
104.0	62.06	0.344	0.86	1.0	2.14	32.4
122.0	61.78	0.354	0.85	1.0	2.65	32.4
136.4	61.53	0.362	0.84	1.0	2.90	32.4
(0.75% sol'n by weight; pH = 3.0)						
49.8	62.58			1.00	0.49	
59.0	62.54	0.312	0.79	1.00	0.85	95
70.2	62.50	0.318	0.77	1.00	1.20	109
86.5	62.34	0.326	0.74	1.00	1.70	129
105.8	62.12	0.336	0.70	1.00	2.23	153
123.8	61.87	0.341	0.67	1.00	2.65	175
141.0	61.46	0.353	0.64	1.00	3.02	195
(1.0% sol'n by weight; pH = 3.0)						
50.0	62.62		0.60	1.0	0.50	510
75.2	62.49	0.309	0.44	1.0	1.35	973
86.0	62.39	0.313	0.41	1.0	1.70	1390
104.0	62.19	0.320	0.35	1.0	2.15	1500
122.0	61.91	0.326	0.29	1.0	2.60	1860

Table 12  
Physical Properties of Methocel Solution 1%

$t$ $^{\circ}\text{F}$	$\text{lb}_M/\text{ft}^3$	$K$ $\text{lb}_M/\text{ft}\cdot\text{hr}^{2-N}$	$n$ Flow Index	$k$ $\text{Btu}/\text{hr}\cdot\text{ft}(\text{F})$	$C_P$ $\text{Btu}/\text{lb}_M\text{F}$	$\beta$ $\times 10^4$ $^{\circ}\text{R}^{-1}$
59.0	62.52	39.4	0.99	0.314	1.0	0.82
68.0	62.49	27.8	0.98	0.317	1.0	1.25
86.0	62.37	19.7	0.97	0.326	1.0	1.70
104.0	62.20	15.1	0.95	0.331	1.0	2.15
122.0	61.97	12.8	0.93	0.337	1.0	2.60

Table 13  
Physical Properties of Carbose I.M. 0.5%

$t$ $^{\circ}\text{F}$	$\text{lb}_M/\text{ft}^3$	$K$ $\text{lb}_M/\text{ft}\cdot\text{hr}^{2-N}$	$n$ Flow Index	$k$ $\text{Btu}/\text{hr}\cdot\text{ft}(\text{F})$	$C_P$ $\text{Btu}/\text{lb}_M\text{F}$	$\beta$ $\times 10^4$ $^{\circ}\text{R}^{-1}$
68	62.47	35.9	0.88	0.326	1.0	1.25
86	62.31	27.2	0.88	0.335	1.0	1.70
104	62.11	23.2	0.88	0.344	1.0	2.15
122	61.83	19.7	0.88	0.354	1.0	2.60

Table 14  
 Flow Curve Data: 1% Carbopol Sol'n  
 Spindle No. 1: pH = 3.00

N Rpm	R %	$\tau_i^*$ $\times 10^2$	$-\left(\frac{du}{dr}\right)_i^*$	N Rpm	R %	$\tau_i$ $\times 10^{+3}$	$-\left(\frac{du}{dr}\right)_i$
T=20.7°C; m=2.28; n=0.45; K=7.7x10 <sup>-3</sup>				T=10.0°C; m=1.71; n=0.60; K=4.4x10 <sup>-3</sup>			
0.3	10.3	0.338	0.143	1.5	9.4	3.08	0.536
0.6	13.7	0.449	0.286	3	13.7	4.49	1.07
1.5	20.0	0.656	0.715	6	20.8	6.82	2.14
3	26.8	0.879	1.43	12	31.2	10.2	4.29
6	36.7	1.20	2.86	30	54.1	17.7	10.7
12	51.0	1.67	5.72	60	83.0	27.2	21.4
30	81.1	2.66	14.3				
T=25.9°C; m=2.33; n=0.43; K=8.6x10 <sup>-3</sup>				T=30.0°C; m=2.57; n=0.40; K=1.0x10 <sup>-2</sup>			
0.3	12.0	0.394	0.146	0.3	16.8	5.51	0.161
0.6	15.8	0.518	0.292	0.6	20.9	6.86	0.322
1.5	22.5	0.738	0.730	1.5	28.8	9.45	0.806
3	29.8	0.977	1.46	3	36.8	12.1	1.61
6	40.4	1.32	2.92	6	48.4	15.9	3.22
12	55.4	1.82	5.84	12	65.0	21.3	6.44
30	86.1	2.82	14.6	30	97.8	32.1	16.1
T=40°C; m=3.20; n=0.35; K=1.3x10 <sup>-2</sup>				T=50°C; m=3.62; n=0.28; K=1.6x10 <sup>-2</sup>			
0.3	25.8	0.846	0.201	0.3	33.8	11.1	0.227
0.6	30.8	1.01	0.402	0.6	39.1	12.8	0.454
1.5	39.9	1.31	1.00	1.5	50.4	16.5	1.13
3	50.0	1.64	2.01	3	61.1	20.0	2.27
6	63.3	2.08	4.02	6	75.7	24.8	4.54
12	80.9	2.65	8.02	12	95.4	31.3	9.08

\*  $\tau_i$  in lb.<sub>f</sub>/ft.<sup>2</sup>;  $\left(\frac{du}{dr}\right)_i$  in (sec)<sup>-1</sup>; K in lb.<sub>f</sub>/ft.<sup>2</sup> For Tables  
 14 - 18.

Table 15  
Flow Curve Data--0.75% Carbopol Solution  
(Brookfield U.L. Adapter)

Carbopol Solution--0.75% by Weight							
N RPM	R $\times 10^2$	$T_i \times 10^3$ lb <sub>f</sub> /ft <sup>2</sup>	$-(\frac{du}{dr})_i$ (sec) <sup>-1</sup>	N RPM	R $\times 10^2$	$T_i \times 10^3$ lb <sub>f</sub> /ft <sup>2</sup>	$-(\frac{du}{dr})_i$ (sec) <sup>-1</sup>
T=71.0°F; m=1.29; n=0.77; K=0.94 $\times 10^{-3}$				T=88.3°F; m=1.38; n=0.73; K=1.15 $\times 10^{-3}$			
0.3				0.3	4.0	0.62	0.40
0.6	5.1	0.78	0.80	0.6	6.3	0.97	0.81
1.5	10.2	1.57	2.01	1.5	12.4	1.91	2.02
3	17.5	2.70	4.02	3	20.7	3.19	4.05
6	30.3	4.67	8.04	6	34.5	5.31	8.10
12	52.0	8.01	16.1	12	57.5	8.86	16.2
T=105.8°F; m=1.43; n=0.71; K=1.30 $\times 10^{-3}$				T=123.5°F; m=1.57; n=0.67; K=1.50 $\times 10^{-3}$			
0.3	4.6	0.71	0.41	0.3	5.5	0.85	0.41
0.6	7.4	1.14	0.82	0.6	8.2	1.26	0.82
1.5	14.0	2.16	2.04	1.5	15.4	2.37	2.06
3	22.6	3.48	4.08	3	24.0	3.70	4.11
6	37.2	5.73	8.16	6	38.5	5.93	8.22
12	60.8	9.36	16.3	12	62.1	9.56	16.4

ASSUMPTION UNIVERSITY LIBRARY

Flow Curve Data  
Carbopol Solution--0.50% by Weight

N	$R \times 10^2$	$\tau_i$	$-\left(\frac{du}{dr}\right)_i$	N	$R \times 10^2$	$\tau_i$	$-\left(\frac{du}{dr}\right)_i$
$T=59^\circ F; m=1.10; n=0.89; K=0.275 \times 10^{-3}$				$T=68^\circ F; m=1.12; n=0.89; K=0.275 \times 10^{-3}$			
3	6.1	0.94	3.96	3	6.1	0.94	3.96
6	11.6	1.79	7.92	6	11.6	1.79	7.92
12	21.4	3.30	15.8	12	21.4	3.30	15.8
30	48.5	7.47	39.6	30	48.0	7.39	39.6
60	89.9	13.8	79.2	60	88.6	13.6	79.2
$T=86^\circ F; m=1.14; n=0.88; K=0.280 \times 10^{-3}$				$T=104^\circ F; m=1.17; n=0.86; K=0.280 \times 10^{-3}$			
3	6.1	0.94	3.96	3	6.0	0.92	3.99
6	11.5	1.77	7.92	6	11.0	1.69	7.98
12	20.8	3.20	15.8	12	20.1	3.10	16.0
30	46.2	7.11	39.6	30	43.6	6.71	39.9
60	84.2	13.0	79.2	60	79.2	12.2	79.8
$T=122^\circ F; m=1.18; n=0.85; K=0.280 \times 10^{-3}$							
3	5.6	0.86	3.99				
6	10.3	1.59	7.98				
12	18.5	2.85	16.0				
30	40.3	6.21	39.9				
60	72.8	11.2	79.8				



Table 17  
Flow Curve Data: 1% Methocel Solution

$T = 22.4^{\circ}\text{C}/72.3^{\circ}\text{F}$ $m = 1.03$ $N = 0.98$ $K = 0.22 \times 10^{-3}$				
N Rpm	R $\times 10^2$	L	$\tau_i$	$-(\frac{du}{dr})_i$
3	5.2	3.62	$0.80 \times 10^{-3}$	3.93
6	10.1	3.62	1.55 "	7.86
12	19.5	3.62	3.00 "	15.7
30	48.3	3.62	7.44 "	39.3
60	96.7	3.62	14.8 "	78.6

$T = 29.7^{\circ}\text{C}/85.4^{\circ}\text{F}$ $m = 1.03$ $n = 0.97$ $K = 0.17 \times 10^{-3}$				
N Rpm	R $\times 10^2$	L	$\tau_i$	$-(\frac{du}{dr})_i$
3	4.2	3.62	$0.65 \times 10^{-3}$	3.93
6	7.9	3.62	1.22 "	7.86
12	15.2	3.62	2.34 "	15.7
30	37.6	3.62	5.79 "	39.3
60	75.7	3.62	11.6 "	78.6

$T = 45.1^{\circ}\text{C}/113.2^{\circ}\text{F}$ $m = 1.05$ $n = 0.94$ $K = 0.12 \times 10^{-3}$				
N Rpm	R $\times 10^2$	L	$\tau_i$	$-(\frac{du}{dr})_i$
6	5.4	3.62	$0.83 \times 10^{-3}$	7.92
12	10.4	3.62	1.60 "	15.8
30	23.8	3.62	3.66 "	39.6
60	47.5	3.62	7.32 "	79.2

$T = 20.9^{\circ}\text{C}/69.6^{\circ}\text{F}$ $m = 1.02$ $N = 0.98$ $K = 0.24 \times 10^{-3}$				
N Rpm	R $\times 10^2$	L	$\tau_i$	$-(\frac{du}{dr})_i$
1.5	3.3	3.62	$0.51 \times 10^{-3}$	1.97
3	6.0	3.62	0.925 "	3.93
6	11.8	3.62	1.82 "	7.86
12	23.2	3.62	3.58 "	15.7
30	57.3	3.62	8.84 "	39.3

Table 18  
Flow Curve Data--0.5% Carbose Sol'n

N RPM	$R \times 10^2$	$T_i \times 10^3$	$(-\frac{du}{dr})_{\text{sec}^{-1}}$
Temp = 20.0°C/68°F    m = 1.16    n = 0.88    K = 3.1x10 <sup>-4</sup>			
1.5	3.8	0.58	1.98
3	6.7	1.03	3.96
6	12.2	1.88	7.92
12	23.0	3.54	15.8
30	54.2	8.35	39.6
60	99.8	15.4	79.2
Temp = 30°C/86°F    m = 1.12    n = 0.88    K = 2.35x10 <sup>-4</sup>			
1.5	2.9	0.45	1.98
3	5.1	0.78	3.96
6	9.4	1.45	7.92
12	17.6	2.71	15.8
30	41.0	6.31	39.6
60	79.0	12.2	79.2
Temp = 40°C/104°F    m = 1.13    n = 0.88    K = 2.00x10 <sup>-4</sup>			
1.5	2.5	0.38	1.98
3	4.3	0.66	3.96
6	7.2	1.11	7.92
12	13.5	2.08	15.8
30	31.4	4.84	39.6
60	60.6	9.33	79.2
Temp = 47°C/116.6°F    m = 1.12    n = 0.88    K = 1.70x10 <sup>-4</sup>			
1.5	2.1	0.32	1.98
3	3.6	0.55	3.96
6	6.3	0.97	7.92
12	11.5	1.77	15.8
30	26.7	4.11	39.6
60	51.4	7.00	79.2

APPENDIX V  
HEAT TRANSFER DATA

APPENDIX V

Table No. 19  
Heat Transfer Data - Water

Run	Average Temperature $T_3 - T_4$ - °F	$\Delta T$ (4-3) - °F	Watts	Volts	q corr. q	h BFU/hr ft <sup>2</sup> °F	N <sub>NU</sub>	N <sub>PR</sub>	N <sub>GR</sub> x 10 <sup>-5</sup>	N <sub>Ra</sub> x 10 <sup>-6</sup>
1	71.6	9.9	9.9	37.7	2.4	33.6	8.06	6.67	2.15	1.43
2	80.7	13.8	20.0	53.5	3.9	49.7	11.7	5.84	4.63	2.70
3	56.8	6.5	5.0	26.9	1.2	25.8	6.37	8.90	0.507	0.451
4	64.0	5.9	5.0	26.9	1.5	28.1	6.83	7.46	0.848	0.633
5	88.2	17.5	30.0	65.7	3.3	60.7	14.1	5.29	7.96	4.21
6	87.3	17.4	30.0	65.7	3.3	61.0	14.2	5.37	7.60	4.08
7	66.5	7.5	7.6	33.0	1.8	34.4	8.32	7.18	1.26	0.904
8	100.4	18.9	34.8	71.0	5.8	63.8	14.7	4.52	13.3	6.03
9	99.1	21.2	40.1	76.1	6.5	65.8	15.1	4.60	14.3	6.57
10	74.9	11.7	14.9	43.0	3.0	44.0	10.5	6.35	3.01	1.91
11	83.9	16.3	25.2	60.2	4.6	56.2	13.2	5.60	6.25	3.50
12	64.6	11.1	10.0	37.4	2.8	30.2	7.32	7.40	1.65	1.22
13	65.7	11.3	10.0	37.4	2.9	29.5	7.13	7.30	1.79	1.31
14	60.6	8.5	7.5	32.3	2.1	29.4	7.18	7.95	0.992	0.789
15	81.3	12.5	15.0	46.4	2.4	46.9	10.5	5.87	4.19	2.46
16	79.0	16.0	20.0	53.5	3.0	48.9	11.6	6.04	4.90	2.96
17	83.5	19.0	25.0	60.0	3.6	51.4	12.1	5.75	6.68	3.84
18	102.2	21.5	35.0	71.2	4.1	63.7	14.6	4.45	15.9	7.09
19	92.2	24.5	41.0	72.2	4.7	65.4	15.2	5.00	13.0	6.48
20	88.0	28.0	40.0	76.0	5.3	55.9	13.0	5.31	12.5	6.64
21	64.0	12.1	10.0	37.4	1.9	32.5	7.89	7.47	1.71	1.28
22	70.8	6.5	5.0	26.9	1.2	30.1	7.20	6.74	1.37	0.925

For location of thermocouples see Figure 10, Appendix VII

Table No. 20  
Heat Transfer Data - Glycerine

Run	Average Plate Temperature	$\Delta T$ (4-3) - °F	Heat Input				h BTU/hr ft <sup>2</sup> °F	N <sub>NU</sub>	N <sub>PR</sub>	N <sub>GR</sub>	N <sub>Ra</sub> x 10 <sup>-4</sup>
	3 & 4 - °F		Watts	Volts	q corr.	q					
1	88.0	43.5	15.0	46.5	7.9	40.5	10.5	5.30	4,900	9.55	4.68
2	84.9	41.1	12.5	41.8	7.5	36.1	9.94	5.02	5,650	7.61	4.30
3	69.8	21.4	5.1	26.7	3.7	12.8	6.77	3.42	11,500	7.81	0.978
4	74.1	29.0	7.5	32.3	5.2	19.0	7.42	3.74	9,200	1.78	1.64
5	79.2	36.3	10.2	37.8	6.6	26.4	8.23	4.16	7,300	3.63	2.65
6	81.1	34.4	11.1	39.6	6.1	29.7	9.77	4.93	6,600	4.11	2.71
7	87.8	46.2	16.1	48.0	8.4	43.6	10.7	5.41	4,900	10.1	4.97
8	92.8	52.2	19.0	52.2	9.6	51.7	11.2	5.65	4,000	19.6	7.85
9	97.6	56.5	22.5	57.0	10.5	62.1	12.4	6.26	3,300	33.6	11.1
10	72.4	19.8	5.1	26.7	3.6	12.9	7.38	3.73	10,000	1.03	1.03
11	81.8	34.0	10.2	37.8	6.2	26.8	8.79	4.44	6,350	4.39	2.79
12	91.3	40.6	15.2	46.6	7.4	41.7	11.6	5.86	4,260	13.0	5.52
13	94.4	51.4	19.9	58.5	9.5	54.0	11.9	6.01	3,750	22.7	8.50
14	100.4	57.9	23.5	58.0	10.8	65.1	12.7	6.41	2,900	43.8	12.7
15	70.6	12.8	2.5	18.8	2.3	5.8	5.13	2.59	11,100	0.550	0.610
16	73.7	12.4	3.0	21.0	2.2	7.5	6.85	3.46	9,400	0.747	0.702
17	75.7	20.6	6.0	28.7	2.8	16.6	9.12	4.60	8,500	1.52	1.29
18	88.2	41.3	14.9	46.4	7.8	40.3	11.0	5.56	4,900	9.16	4.49
19	90.0	45.0	17.5	50.2	8.6	47.9	12.0	6.06	4,550	12.2	5.57
20	94.0	50.0	20.0	53.5	9.5	55.1	12.5	6.32	3,800	21.2	8.04
21	106.5	65.0	25.2	60.2	12.4	69.0	12.0	6.06	2,270	87.7	19.9
22	98.5	55.0	22.5	57.0	10.3	62.3	12.8	6.46	3,150	35.6	11.2
23	66.6	8.9	1.5	14.7	1.7	3.2	3.94	1.99	13,000	0.253	0.329
24	66.4	10.7	2.0	17.0	1.9	4.6	4.83	2.44	13,000	0.309	0.402
25	67.3	14.0	2.5	19.0	2.5	5.7	4.61	2.33	12,800	0.430	0.550
26	66.0	7.5	1.0	11.5	1.3	1.9	2.87	1.45	13,200	0.204	0.269
27	65.4	10.4	1.5	14.6	1.6	3.2	3.43	1.73	13,200	0.283	0.364
28	67.2	11.8	2.5	18.8	2.1	6.1	5.84	2.95	12,800	0.368	0.471
29	69.0	16.8	4.1	24.0	3.0	10.2	6.88	3.48	11,900	0.621	0.739
30	64.6	7.5	1.0	11.0	1.4	1.8	2.72	1.38	13,800	0.179	0.247
31	64.7	8.9	1.5	14.4	1.6	3.2	4.07	2.06	13,700	0.222	0.304
32	65.8	10.5	2.1	17.0	1.8	5.0	5.39	2.72	13,200	0.285	0.376

Table No. 21

Heat Transfer Data - 1.0% Methocel

Run	Average Plate Temperature	$\Delta T$ (4-3) - °F	Heat Input				h Btu/hr ft <sup>2</sup> °F	N <sub>NU</sub>	N <sub>PR</sub>	N <sub>GR</sub>	N <sub>Ra</sub> x 10 <sup>-5</sup>
	3 & 4 - °F		Watts	Volts	q corr.	q					
1	72.8	5.1	2.6	19.6	1.0	7.4	16.5	4.31	74.0	1,140	0.844
2	67.8	8.5	5.0	26.8	1.6	12.5	19.4	5.10	85.6	1,240	1.06
3	65.0	12.7	7.6	33.0	2.4	22.1	19.7	5.19	92.9	1,380	1.28
4	68.8	13.1	10.1	38.1	2.5	29.3	25.3	6.65	86.7	1,950	1.69
5	72.2	17.6	12.5	42.3	3.3	37.0	23.8	6.21	75.8	3,580	2.75
6	74.6	18.8	15.0	46.6	3.6	44.8	27.0	7.03	70.5	4,780	3.37
7	77.7	20.9	17.5	50.1	4.0	52.6	28.5	7.40	65.3	6,610	4.32
8	80.0	22.0	20.0	53.7	4.2	60.4	31.1	8.04	61.0	8,270	5.04
9	75.6	7.3	5.0	26.8	1.4	14.8	22.9	5.96	69.1	2,000	1.38
10	92.0	24.7	25.0	60.0	4.7	76.0	34.8	8.89	46.2	18,600	8.59
11	92.0	27.0	27.6	63.1	5.1	83.9	35.2	8.99	46.2	20,300	9.36
12	94.2	28.5	30.0	65.8	5.4	91.4	36.3	9.25	45.7	22,600	10.3

**Table No. 22**  
**Heat Transfer Data - 0.5% Carbopol**

Run	Average Plate Temperature 3 4 - °F	$\Delta T$ (4-3) - °F	Watts	Volts	Heat Input q corr.	q	h BTU/hr ft <sup>2</sup> °F	N <sub>NU</sub>	N <sub>PR</sub>	N <sub>GR</sub>	N <sub>Ra</sub> x 10 <sup>-5</sup>
1	64.8	10.3	5.0	26.4	2.2	14.0	15.4	3.95	65.1	2,320	1.51
2	64.8	11.7	7.5	32.7	2.6	21.6	20.9	5.37	65.3	2,640	1.73
3	70.6	16.7	12.5	42.5	3.9	36.4	24.7	6.29	64.8	4,320	2.80
4	77.0	20.7	17.7	50.5	5.1	52.0	28.4	7.17	62.0	6,710	4.16
5	69.2	14.5	10.0	37.7	3.2	29.1	22.7	5.80	64.8	3,660	2.37
6	74.6	18.5	15.1	46.6	4.3	44.5	27.2	6.89	62.0	5,680	3.52
7	79.2	22.4	20.0	53.8	5.3	59.2	29.9	7.53	61.7	7,640	4.71
8	79.8	20.7	16.7	48.9	4.6	49.3	27.0	6.78	61.7	7,180	4.43
9	84.0	24.1	22.5	57.1	5.5	67.2	31.6	7.88	61.0	8,320	5.08
10	79.4	21.2	19.0	52.3	4.9	56.4	30.1	7.56	61.7	7,350	4.53
11	78.9	21.2	16.5	48.5	4.5	48.8	26.0	6.54	61.7	7,230	4.46
12	86.4	26.3	25.8	61.0	6.2	77.1	33.2	8.26	61.0	10,200	6.22
13	82.8	24.0	22.5	57.0	5.6	67.1	31.6	7.90	51.4	8,870	5.45
14	89.8	28.9	30.0	65.8	6.8	90.0	35.2	8.70	58.7	12,800	7.51
15	92.2	30.5	32.5	68.5	7.3	97.6	36.2	8.92	58.4	13,900	8.12
16	88.0	26.9	27.7	63.2	6.3	83.1	35.0	8.68	60.7	10,700	6.49
17	96.2	33.5	35.1	71.4	8.0	105.2	35.5	8.70	58.1	16,000	9.30
18	89.1	30.4	30.0	65.7	7.8	89.0	33.1	8.18	58.7	13,300	7.81
19	62.2	9.9	4.7	25.5	2.1	13.1	15.0	3.88	65.8	2,020	1.33
20	64.6	12.5	7.5	32.7	2.8	21.4	19.4	4.99	65.1	2,750	1.79
21	67.7	15.2	11.1	39.7	3.5	32.3	24.0	6.06	65.1	3,670	2.39
22	63.8	11.7	6.3	30.0	2.5	17.9	17.3	4.46	65.1	2,510	1.63
23	68.2	14.5	10.7	39.0	3.2	31.4	24.5	6.28	65.1	3,580	2.33
24	76.2	20.5	18.6	52.0	4.7	55.4	30.6	7.73	62.0	6,290	3.90
25	79.6	23.2	21.2	55.3	5.4	62.9	30.4	7.70	61.7	8,040	4.96
26	82.0	25.1	22.5	57.0	5.8	66.9	30.2	7.56	61.4	1,130	5.60
27	86.2	28.1	27.0	62.6	6.5	80.6	32.5	8.08	61.0	10,900	6.65

Table No. 23  
Heat Transfer Data - 0.50% Carbose

Run	Average Plate Temperature $T_p$ - °F	$\Delta T$ (4-3) - °F	Watts	Volts	Heat Input q corr. q	h Btu/hr ft <sup>2</sup> °F	$N_{NU}$	$N_{PR}$	$N_{GR}$	$N_{Ra}$ $\times 10^{-5}$
1	82.0	20.1	15.0	46.0	4.3	44.2	6.22	55.3	7,860	4.33
2	86.8	22.9	20.2	53.7	5.1	60.1	7.39	51.8	11,700	6.07
3	79.0	17.8	12.5	42.1	3.9	36.4	5.82	57.7	6,480	3.74
4	82.5	21.2	17.5	50.0	4.7	51.8	6.92	54.9	8,940	4.91
5	91.1	26.3	25.0	60.2	6.0	74.6	7.94	49.2	15,500	7.63
6	73.3	12.8	7.3	31.9	2.6	21.0	4.72	62.2	3,570	2.22
7	74.8	16.1	10.1	37.7	3.2	29.4	5.24	61.9	4,880	3.02
8	75.5	17.5	11.6	40.5	3.6	34.0	5.58	61.7	5,400	3.33
9	89.1	29.0	27.5	63.0	6.6	82.2	7.94	51.2	15,600	8.00
10	89.3	25.1	22.7	57.2	5.5	68.0	7.57	51.2	13,500	6.90
11	95.6	29.8	30.0	65.7	6.8	90.0	8.38	47.9	19,700	9.44
12	98.8	33.0	35.2	71.2	7.7	105.9	8.84	46.0	24,400	11.2
13	77.7	18.8	13.5	43.8	4.0	39.6	6.01	61.2	5,570	3.41
14	81.2	29.2	10.5	38.5	5.6	28.3	2.76	54.2	12,300	6.67
15	81.8	20.6	15.5	47.2	5.0	45.0	6.20	54.0	8,680	4.69
16	85.9	23.6	20.6	54.5	5.2	61.3	7.31	53.4	9,940	5.31
17	91.5	27.2	26.1	61.4	6.2	78.0	8.01	49.2	16,000	7.87
18	96.2	28.2	29.2	64.8	6.4	87.8	8.62	47.7	18,600	8.87
19	99.0	31.9	34.0	70.0	7.4	102.4	8.84	46.0	23,600	10.8
20	102.0	34.4	37.7	74.0	8.1	113.5	9.06	44.4	27,700	12.3



Table No. 24

Heat Transfer Data - 0.75% Carbopol

Run	Average Plate Temperature $3\frac{1}{4} - 4 - 4 - \text{ } ^\circ\text{F}$	$\Delta T$ (4-3) $^\circ\text{F}$	Watts	Volts q corr.	Heat Input q	h BFU/hr ft <sup>2</sup> $^\circ\text{F}$	N <sub>NU</sub>	N <sub>PR</sub>	N <sub>GR</sub>	N <sub>Ra</sub> $\times 10^{-5}$
1	70.8	22.3	10.0	37.5	4.6	27.7	3.70	123	1,620	1.99
2	76.0	26.7	15.0	46.4	5.6	42.8	4.71	122	2,310	2.82
3	63.4	15.3	5.2	26.9	3.1	13.7	2.68	122	962	1.17
4	82.3	34.2	20.3	53.7	7.3	58.3	4.97	123	3,240	3.98
5	85.2	36.9	22.5	57.0	7.9	64.8	5.08	122	3,710	4.52
6	66.0	18.9	7.6	32.9	3.9	20.7	3.27	123	1,270	1.56
7	74.1	25.6	12.6	42.5	5.3	35.3	4.07	123	2,070	2.54
8	80.8	31.2	17.9	50.6	6.4	51.3	4.80	123	2,880	3.54
9	89.0	42.1	25.2	60.4	8.9	72.4	4.97	121	3,920	4.74
10	92.2	46.9	30.0	65.8	10.0	87.0	5.32	122	5,140	6.28
11	81.8	35.4	19.8	53.5	7.3	56.6	4.65	124	3,270	4.05
12	94.8	44.5	27.7	63.2	9.3	80.2	5.17	121	5,070	6.13
13	100.2	50.0	32.5	68.4	10.6	94.2	5.33	120	6,270	7.52
14	62.4	14.1	4.7	25.5	3.0	12.4	2.64	121	980	1.10
15	70.0	17.9	8.6	35.0	3.8	24.0	3.99	122	1,740	2.12
16	72.0	24.1	12.6	42.5	5.0	35.7	4.39	121	2,340	2.83
17	77.6	28.1	15.2	46.8	5.8	44.7	4.73	123	2,520	3.10
18	82.4	34.3	20.0	53.9	7.2	57.3	4.86	123	3,090	3.80

Table No. 25

Heat Transfer Results - 1% Carbopol

Run	Average Plate Temperature $\frac{3+4}{2} - ^\circ\text{F}$	$\Delta T$ (4-3) - $^\circ\text{F}$	Watts	Volts	q corr.	Heat Input	q	h	B $\dot{T}U/hr$	ft $^2$	$^\circ\text{F}$	N <sub>NU</sub>	N <sub>PR</sub>	N <sub>GR</sub>	N <sub>Ra</sub> $\times 10^{-5}$
1	82.0	44.5	10.0	38.0	8.5	23.8	6.06	1.61	197	1,790	3.53				
2	69.1	26.4	5.0	26.8	5.0	11.1	4.77	1.76	198	811	1.60				
3	74.0	32.9	7.4	32.6	6.2	17.6	6.07	1.64	198	1,120	2.22				
4	68.4	18.5	4.0	24.0	3.5	9.4	5.74	1.56	198	548	1.08				
5	73.8	25.6	7.0	29.4	4.9	17.9	7.92	2.14	198	882	1.75				
6	81.5	36.9	9.1	36.1	7.0	22.4	6.86	1.82	197	1,480	2.92				
7	90.2	51.6	12.3	42.2	9.8	29.9	6.56	1.73	198	2,200	4.36				
8	93.0	62.1	15.0	46.5	11.8	36.6	6.67	1.76	198	2,860	5.66				
9	92.0	64.0	14.9	46.4	12.2	35.9	6.35	1.68	196	3,000	5.88				
10	96.5	71.4	17.5	50.2	13.6	42.9	6.80	1.79	194	3,550	6.89				
11	71.0	22.6	5.0	26.8	4.3	11.9	5.94	1.61	198	734	1.45				
12	83.1	40.8	10.1	38.2	7.3	26.9	7.46	1.98	197	1,560	3.07				
13	97.0	60.7	15.0	46.4	10.1	38.3	7.14	1.88	194	3,020	5.86				

APPENDIX VI  
SAMPLE CALCULATIONS

APPENDIX VI

SAMPLE CALCULATIONS--DIMENSIONLESS GROUPS FOR NON-NEWTONIAN FLUIDS

The generalized dimensionless groups for natural convective heat transfer are the following:

$$\begin{aligned}
 \text{Nusselt Number} \quad N_{Nu} &= \frac{h L}{k} \\
 \text{Prandtl Number} \quad N_{PR} &= \frac{c_p \rho}{k^{N+2}} \left[ \frac{K}{\rho} \right]^{\frac{1}{2-N}} L^{\frac{2N-2}{N-2}} \\
 \text{Grashof Number} \quad N_{GR} &= \frac{L}{\left[ \frac{K}{\rho} \right]^{\frac{2}{2-N}}} g \beta \Delta \theta
 \end{aligned}$$

For the 0.75% Carbopol solution, we have  $h = 14.1$  Btu/hr. (ft<sup>2</sup>)(°F),  $\Delta \theta = 22.3$  F,  $T_{AVG} = 70.8$  F. At 70.8 F,  $n = 0.77$ ;  
 $K = 109$  lb<sub>M</sub>/ft(hr)<sup>2-N</sup>;  $\beta = 1.20 \times 10^{-4}$  °R<sup>-1</sup>;  $c_p = 1.0$  Btu/lb<sub>M</sub>(°F);  
 $k = 0.318$  Btu/(hr)(ft)(°F);  $\rho = 62.50$  lb<sub>M</sub>/ft<sup>3</sup>.

For the Nusselt number:

$$N_{Nu} = \frac{h L}{k} = \frac{14.1 \times 1}{12 \times 0.318} = 3.70$$

For the Prandtl number:

$$\begin{aligned}
 N_{PR} &= \frac{c_p \rho}{k} \left[ \frac{K}{\rho} \right]^{\frac{1}{2-N}} L^{\frac{2N-2}{N-2}} = \frac{(1.0)(62.5)}{(0.318)} \left[ \frac{109}{62.5} \right]^{\frac{1}{2-0.77}} \left[ \frac{1}{12} \right]^{\frac{0.46}{1.23}} \\
 &= (197) [1.75]^{0.813} [0.0833]^{0.374} \\
 &= 197 \times 1.58 \times 0.395 = 123
 \end{aligned}$$

For the Grashof number:

$$N_{GR} = \frac{L^{\frac{N+2}{2-N}} g \beta \Delta \theta}{\left[ \frac{K}{\rho} \right]^{\frac{2.77}{2-N}} \left[ \frac{1}{12} \right]^{1.23} (4.173 \times 10^8) (1.20 \times 10^{-4}) (22.3)}$$

$$= \frac{(0.0833)^{2.26} 1.115 \times 10^6}{(1.75)^{1.63}} = \frac{3.62 \times 10^{-3} \times 1.115 \times 10^6}{2.49}$$

$$N_{GR} = 1620$$

Also  $N_{Ra} = N_{PR} N_{GR} = (1620)(123) = 1.99 \times 10^5$

SAMPLE CALCULATION: FLOW DIAGRAM (0.5% CARBOPOL SOLUTION)

Shearing Stress:  $\tau_i$

Shearing stress at the wall of the inner cylinder is given by:

$$\tau_i = \frac{\text{force}}{\text{area}} = \left( \frac{M}{r_i} \right) \left( \frac{1}{2\pi r_i L} \right)$$

$$\tau_i = M / 2\pi r_i^2 L$$

where  $r_i = 0.0413$  ft.;  $r_i^2 = 1.70 \times 10^{-3}$  ft.<sup>2</sup>;  $M = 4.969 \times 10^{-5}$  S ft-lb.<sub>f</sub>;

S = torque scale reading (B. Vdisc.) (0-1).

$$\text{Thus } \tau_i = \frac{4.969 \times 10^{-5} \times 12}{2\pi \times 1.70 \times 10^{-3}} \left( \frac{S}{L} \right)$$

$$\tau_i = 5.58 \times 10^{-2} \frac{S}{L} \text{ lb.}_f/\text{ft.}^2$$

where L = bob length in inches.

## Shearing Rate

By the method of Krieger and Maron, J.App.Phys., 25, 72:

$$\left(-\frac{du}{dr}\right)_i = \frac{4\pi N}{1-(1/s)^2} \left\{ 1+k_1 \left[ \frac{d \log \phi_s}{d \log F_1} \right] + K_2 \left[ \frac{d \log \phi_s}{d \log F_1} \right]^2 + \frac{k_2 d \left( \frac{d \log \phi_s}{d \log F_1} \right)}{d \log F_1} \right\}$$

$$\text{but } m - 1 = \frac{d \log \phi_s}{d \log F_1}$$

$$\text{where } m = d \log \omega^2 / d \log F_1$$

and

$$\left(-\frac{du}{dr}\right)_i = \frac{4\pi N}{1-1/s^2} \left\{ 1+k_1 \left( \frac{1}{n} - 1 \right) + k_2 \left[ \left( \frac{1}{n} - 1 \right)^2 + \frac{d \left( \frac{1}{n''} - 1 \right)}{d \log M} \right] \right\}$$

where N = rotational speed, rpm.

$$s^2 = (R_i/R_0)^2$$

$$\text{Instrument Constants } \begin{cases} k_1 = \frac{s^2 - 1}{2s^2} \left( 1 + \frac{2}{3} \ln s \right) \\ k_2 = \frac{s^2 - 1}{6s^2} \ln s \end{cases}$$

$n''$  = logarithmic plot of torque M vs. rotational speed N.

$$\phi_s = \text{apparent fluidity} = \frac{4\pi R_1^2 R_2^2 L \omega}{M(R_2^2 - R_1^2)}$$

$$= 2\omega/F_1 \left( 1 - 1/s^2 \right)$$

$$F_1 = \text{Shearing stress at inside cylinder,} = M/2\pi R_1^2 L$$

$$\left(-\frac{du}{dr}\right)_i = \frac{4\pi N}{1 - (1/s^2)} \left\{ 1 + k_1(m-1) + k_2(m-1)^2 + k_2 \frac{d(m-1)}{d \log M} \right\}$$

### Method

- 1) Plot:  $\log N$  vs.  $\log F_1$  and from the slope evaluate  $m$ .
- 2) From the corresponding  $N$ , determine  $\left(-\frac{du}{dr}\right)_i$

### Instrument Constants:

$$k_1 = \frac{s^2 - 1}{2s^2} \left(1 + \frac{2}{3} \ln s\right) = 0.084$$

$$k_2 = \frac{s^2 - 1}{6s^2} \ln s = 0.00229$$

$$s = 1.084/0.991 = 1.094$$

$$\left(-\frac{du}{dr}\right)_i = 78.6 N \left\{ 1 + 0.0843(m-1) + 0.00229(m-1)^2 + 0.00268 \frac{d(m-1)}{d \log M} \right\}$$

### SAMPLE CALCULATION: FLOW DIAGRAM OF 1% CARBOPOL SOLUTION

#### Shearing Stress $\tau_i$

The shearing stress at the wall of the inner cylinder is given by:

$$\tau_i = \frac{M}{2\pi r_i^2 L}$$

- where
- $r_i = 0.3715$  in.
  - $M = 4.969 \times 10^{-5}$  S ft.-lb.<sub>f</sub>
  - $S =$  torque scale reading (0-1.0)
  - $L = 3.02$  inches.

$$\tau_i = \frac{4.969 \times 10^{-5} \times 144 \times 12}{2\pi \times 0.3715^2 \times 3.02} \text{ S lb}_f/\text{ft}^2 = 3.28 \times 10^{-2} \text{ S}$$

Shearing Rate  $(-du/dr)_i$

$$-\left(\frac{du}{dr}\right)_i = \frac{4\pi N}{n''} = 4\pi N m$$

where  $n''$  = the slope of log-log plot of torque  $M$  vs.  $N$  (rotational speed) at the particular  $N$  in question

$m$  = slope of log-log plot of  $N$  vs.  $F_1$

$$-\left(\frac{du}{dr}\right)_i = \frac{4\pi}{60} N m$$

where  $(-\frac{du}{dr})_i = \text{sec}^{-1}$

$N$  = rpm

$m$  = slope of log  $N$  vs. log  $\tau_i$  or  $F_1$

$$\left(-\frac{du}{dr}\right)_i = 0.209 N m (\text{sec}^{-1})$$

#### SAMPLE CALCULATION THERMAL CONDUCTIVITY

According to the basic equation for heat conductivity, the amount of heat per unit time ( $W$ ) flowing through a layer of known geometrical dimensions is proportional to the temperature difference ( $\Delta T$ ) of the two interfaces of the layer and to the thermal conductivity ( $k_M$ ) of the medium. Thus  $W = A k_t \Delta T$  where  $A$  is the proportionality factor which is dependent upon the geometrical dimensions of the layer,



and which might be considered as an apparatus constant. For our cylindrical arrangement, the above equation is true, but A assumes different physical importance than for plain layers. Applying this equation to our experimental arrangement, we have to compile the overall heat flow from the heating block by adding the various parallel portions of the different parts of the liquid layer and the small losses through the centering rods and capillary tubing. Due to the high thermal conductivity of copper the interface temperatures may be considered uniform, even with slightly different densities of heat flow.

Since the heat losses are independent of the kind of liquid under test, it follows that there is a linear relationship between  $W/\Delta T$  and  $k_M$  with two apparatus constants A and B:

$$\frac{W}{\Delta T} = A k_M + B$$

Using redistilled water and a 20% ethylene glycol solution, the apparatus constants A and B were determined for the full temperature range of the tests (Appendix II).

For the 0.75% Carbopol 934 solution at 42 C:

$$W = EI = 0.6373 \text{ watts}$$

$$\Delta T = 1.32 \text{ }^\circ\text{C}$$

and

$$W/\Delta T = 0.4828 \text{ watts/ }^\circ\text{C}$$

At 42°C the apparatus constants are:  $A = 2.552$ ;  $B = -0.3727$

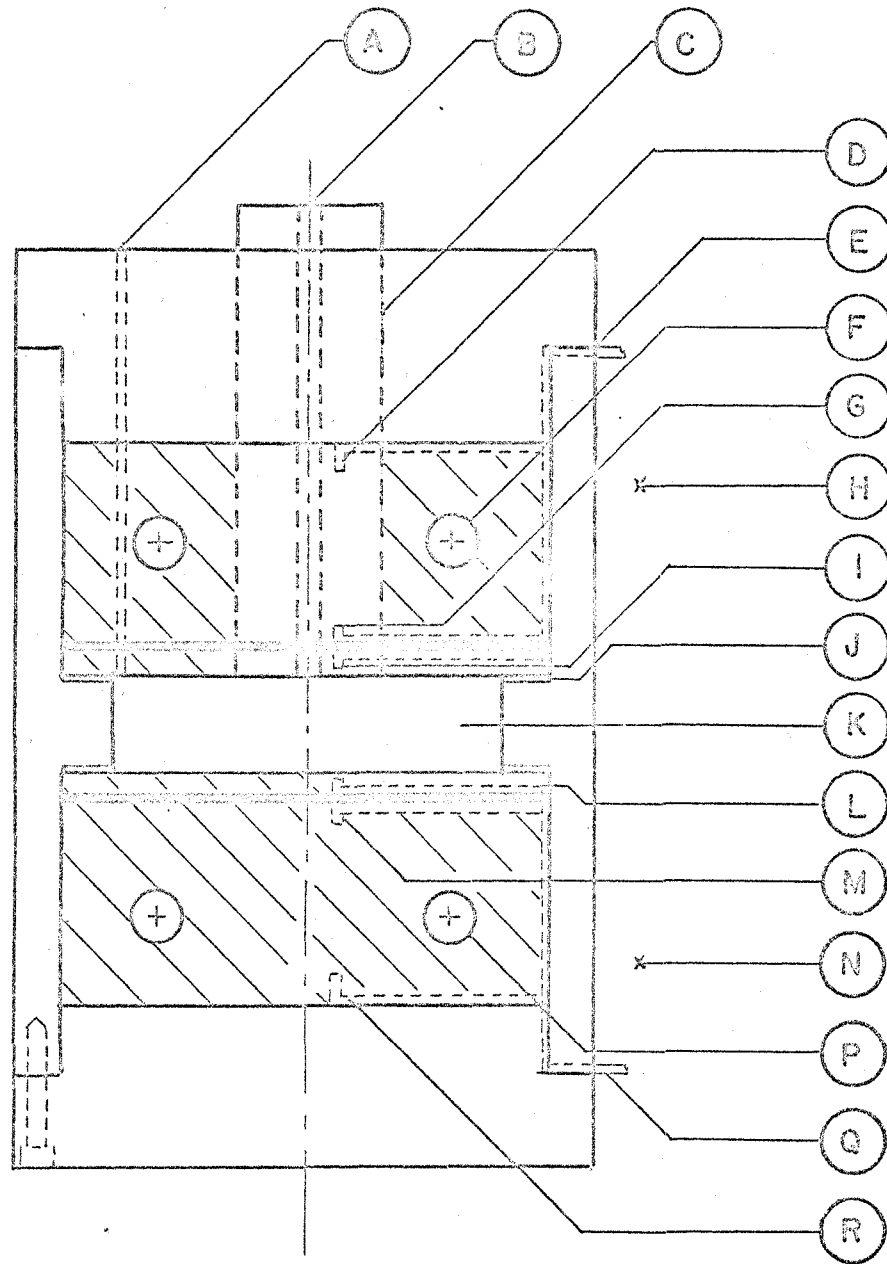
Thus

$$0.4828 = k_M(2.552) - 0.3727$$

$$k_M = \frac{.8535}{2.552} = 0.334 \frac{\text{Btu}}{\text{hr.ft.}(\text{°F})}$$

APPENDIX VII

EXPERIMENTAL EQUIPMENT AND SPECIFICATIONS



COPPER  
  BAKELITE  
  PLEXIGLASS  
 ( HALF SCALE )

FIG.10. DETAIL OF HEAT TRANSFER APPARATUS

## HEAT TRANSFER APPARATUS DETAIL

<u>Symbol</u>	<u>Description</u>
A	Air vent -- liquid container
B	Filling vent
C	Plexiglass Tube
D	Thermocouple No. 1
E	Thermocouples -- Out
F	Cold Water Connection
G	Thermocouple No. 2
H	Thermocouple No. 8
I	Thermocouple No. 3
J	"O"-Ring Seal
K	Liquid Container
L	Thermocouple No. 4
M	Thermocouple No. 5
N	Thermocouple No. 7
P	Heater
Q	Thermocouples -- Out
R	Thermocouple No. 6

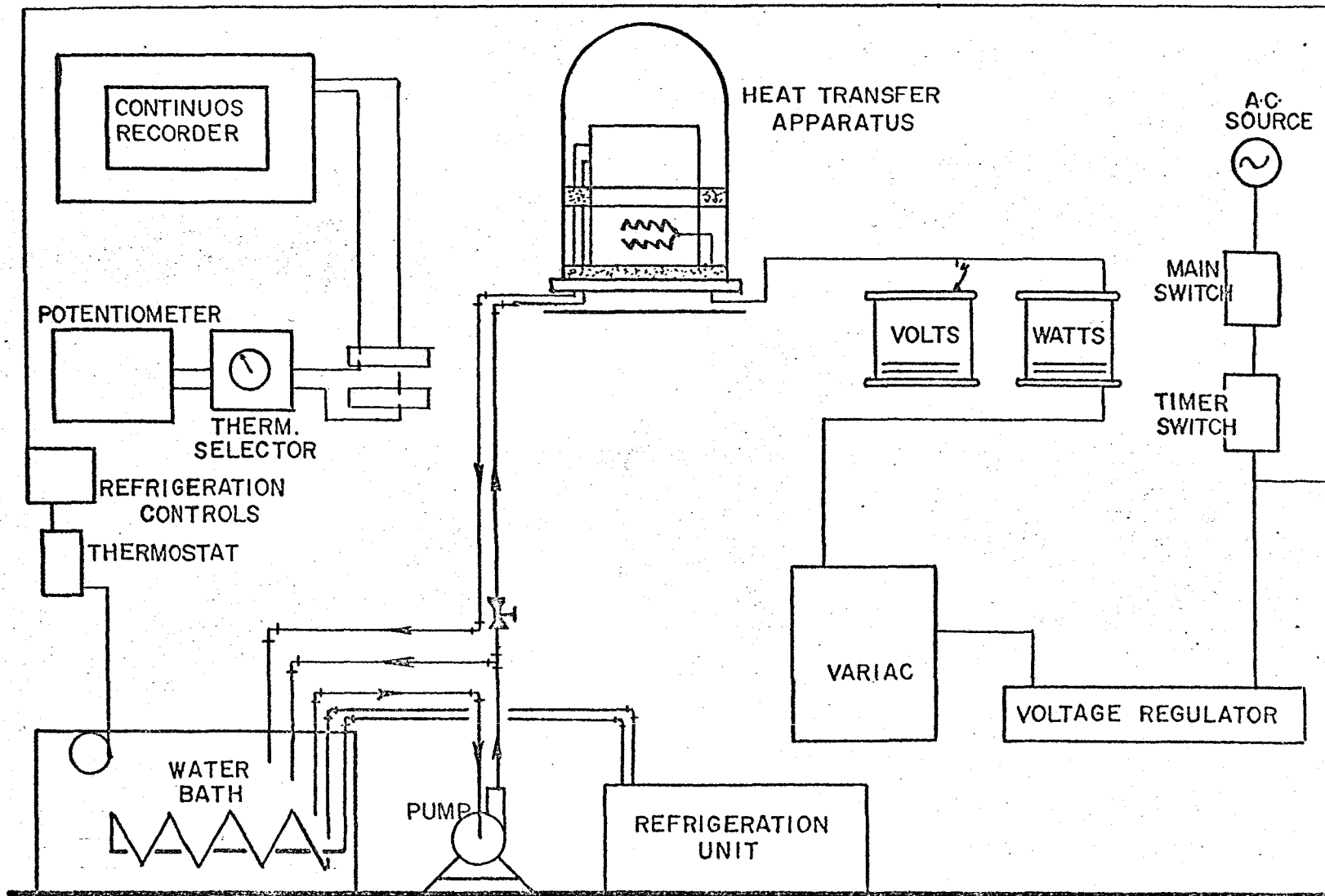


FIG. 11 SCHEMATIC — HEAT TRANSFER SETUP

**EXPERIMENTAL EQUIPMENT AND SPECIFICATIONS**  
**HEAT TRANSFER APPARATUS**  
 (see Fig.11)

- Main Switch:** Double Fuse, 115/230 A.C. volts, Max. Amps. 30
- Time Switch:** General Electric, Type TSA-47, Single-pole, Double Throw
- Contact Rating:** 240 volts A.C.; 35 amps.
- A.C. Voltage Regulator:** Perkin Electronics Corporation, Model MTLR 1000 - 1 K.V.A.  
 A.C. Input: 95-135v, 60 cps  $\pm 10\%$ , 1 phase  
 A.C. Output: 110 - 120 v  
 Accuracy:  $\pm 0.2\%$  for line changes from 105-125 v.  
 Response Time: 0.05-0.1 seconds for line or load changes  
 Load Range: 0 - 8.5 amps.
- Variac Autotransformer:** General Radio Company  
 Type: W20 - G2M  
 Input: 115 volts, 50-60 cps  
 Output: 0-135 volts, 20 amps, 3 K.V.A. Max.
- Wattmeter:** Daystrom, Inc., Weston Instruments Division  
 Accuracy: 0.5% of full scale value  
 Voltage: 75/150 volts  
 Amperage: 1/2 amps  
 Temperature Influence: 0.25% of full scale value  
 from 59 F to 95 F
- Voltmeter:** Daystrom Inc., Weston Instruments Division  
 Model: 904, No. 15113  
 Voltage Range: 75/150 volts  
 Accuracy: 0.5% of full scale value
- Continuous Temperature Recorder:** Daystrom-Weston Industrial Div.  
 Model: 6702, Type 1; Serial 203711  
 Range: 30-160°F, Type T
- Precision Millivolt Potentiometer:** Leeds and Northrup ,  
 Model: 8686  
 Range: -10.1 mv to + 100.1 mv.  
 Limits of Error:  $\pm 0.05\% + 6 \mu v$ .
- Thermocouple Rotary Selector Switch:** Wheelco Instruments  
 Model: 810, 12 T.C. Connections

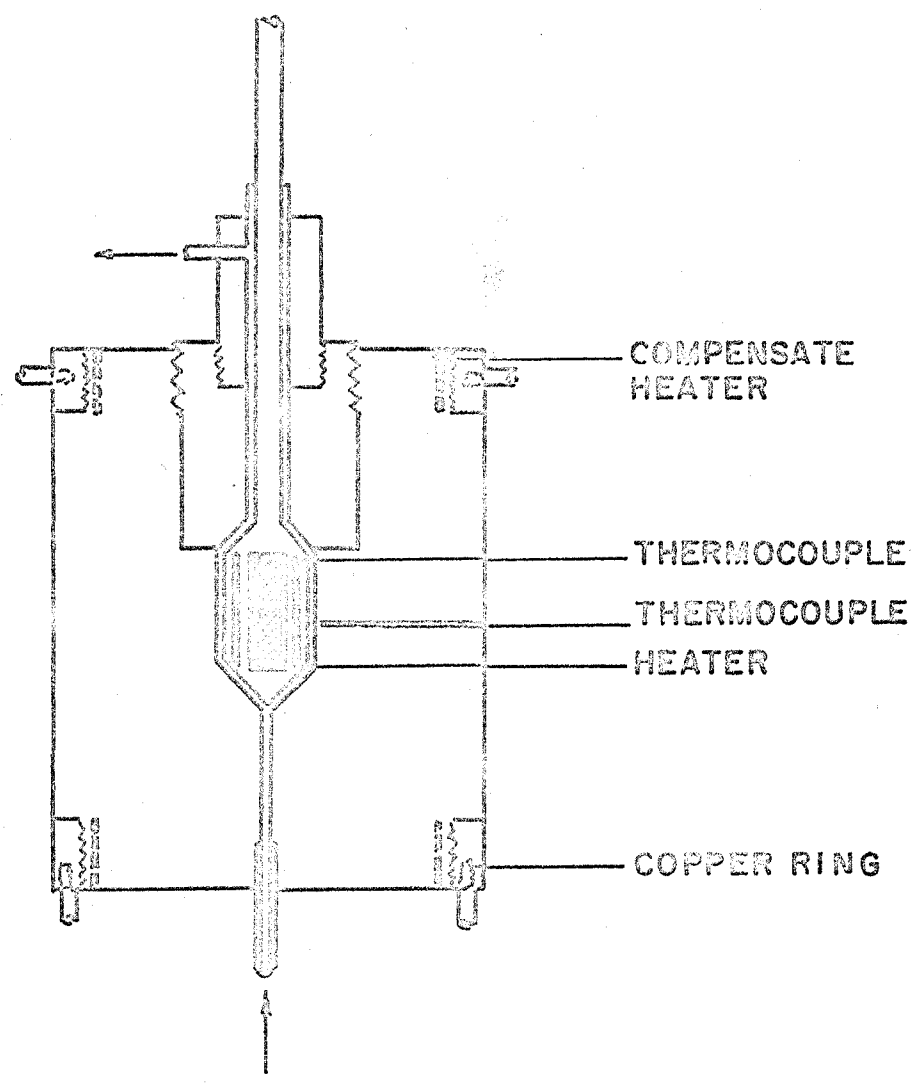


FIG.12 DETAIL OF THERMAL CONDUCTIVITY APPARATUS



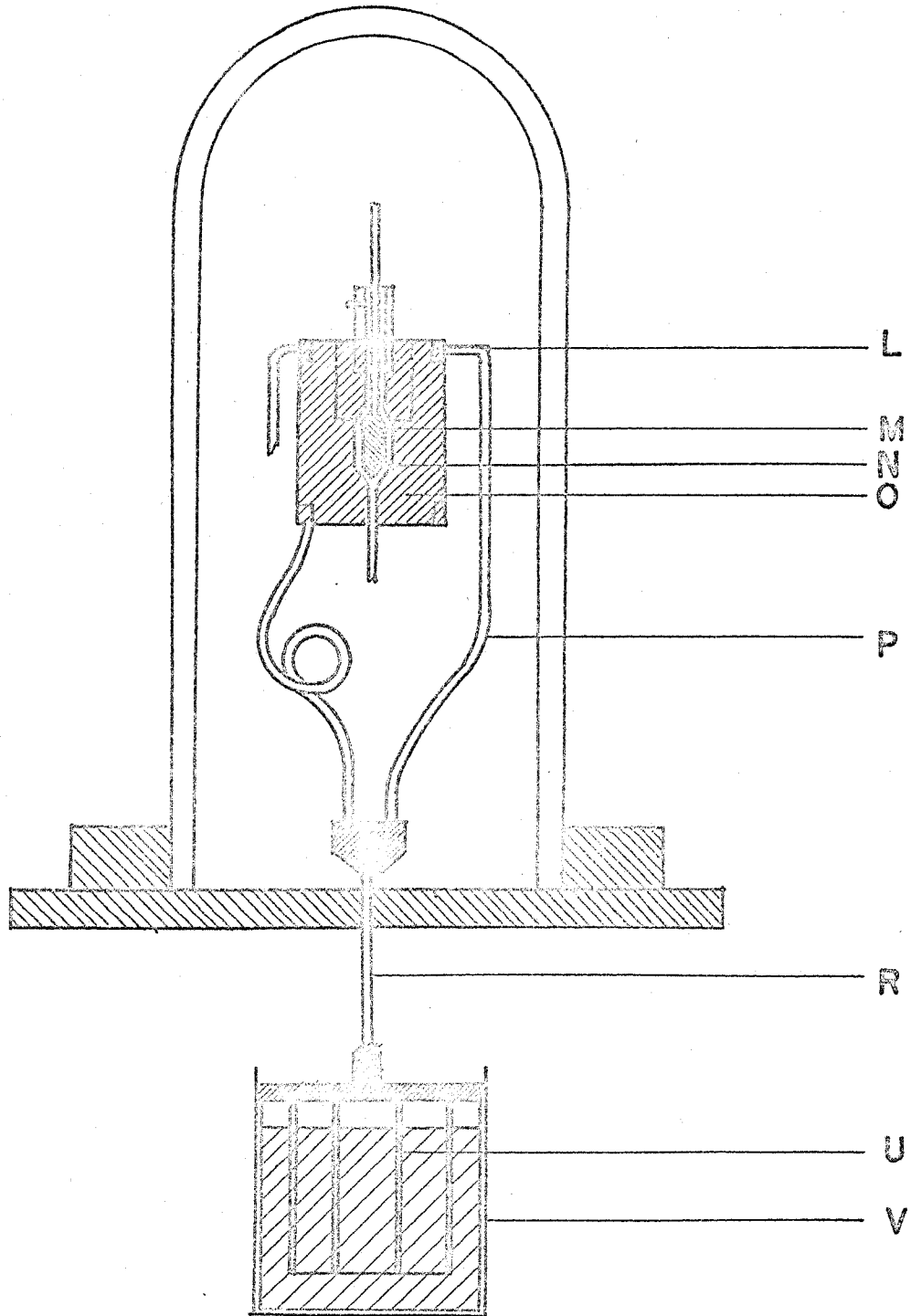


FIG. 13 SCHEMATIC OF EXPERIMENTAL  
THERMAL CONDUCTIVITY SETUP

THERMAL CONDUCTIVITY APPARATUS DETAIL  
(Fig. 13)

<u>Symbol</u>	<u>Description</u>
L	Compensating Heating Element
M	Electrical Heating Source
N	Annular liquid gap
O	Cooling Block
P	Copper Cooling Coils (12)
R	Single Copper Cooling Coil
U	Copper Cylinder
V	Ice-Water Mixture

VITA AUCTORIS

- 1938 Born Carl Clifford St. Pierre on May 12, in Windsor, Ontario, Canada.
- 1952 Completed elementary education at St. Clare's Separate School, Windsor, Ontario, Canada.
- 1956 Completed secondary education at Assumption High School, Windsor, Ontario, Canada.
- 1957 Completed upper school (fifth form) at Assumption High School.
- 1959 Awarded Naval Officers' Association Scholarship as Best Overall Cadet, University Naval Training Division, H.M.C.S. Hunter.
- 1959 Employed as summer assistant in Quality Control Laboratory, Brunner Mond Co., Ltd., Amherstburg, Ontario, Canada.
- 1960 Commissioned in Royal Canadian Navy (Reserve) as Acting Sub-Lieutenant (Ordnance).
- 1961 Graduated from Essex College, Assumption University of Windsor, with the degree of B.A.Sc. in Chemical Engineering.
- 1961 Awarded Board of Governors' Gold Medal in Chemical Engineering.
- 1961 Employed as Chemical Engineer with Hiram Walker and Son's Ltd., Walkerville, Ontario, Canada.
- 1961 Accepted into the Graduate School of Assumption University as candidate for the degree of M.A.Sc. in Chemical Engineering.
- 1962 Awarded Dow Fellowship and accepted into the Graduate School of Northwestern University, Illinois, U.S.A. as candidate for the degree of Ph.D. in Chemical Engineering.